Surface Transporters and Receptors are downregulated by a two-tier system in response to diverse stimuli in *Saccharomyces cerevisiae*

Charlotte Golden

A Thesis
in
The Department
of
Biology

Presented in Partial Fulfillment of the Requirements
for the Degree of Master of Science (Biology) at
Concordia University
Montreal, Quebec, Canada

CONCORDIA UNIVERSITY
School of Graduate Studies

This is to certify that the thesis prepared

By: Charlotte Golden

Entitled: Surface Transporters and Receptors are downregulated by a two-tier system in response to diverse stimuli in *Saccharomyces cerevisiae*

and submitted in partial fulfillment of the requirements for the degree of

Master of Science (Biology)

complies with the regulations of the University and meets the accepted standards with respect to originality and quality

Signed by the final Examining Committee:

_____ Chair
Laurent Potvin-Trottier, PhD

_____ Examiner
Malcolm Whiteway, PhD

_____ Co-supervisor
Alisa Piekny, PhD

_____ Co-supervisor
Christopher L. Brett, PhD

Approved by _____
Robert Weladji, PhD
Graduate Program Director

March 30 2021 _____
Pascale Sicotte, PhD
Dean of the Faculty of Arts and Science

ABSTRACT

Surface Transporters and Receptors
are downregulated by a two-tier system
in response to diverse stimuli in *Saccharomyces cerevisiae*

Charlotte Golden

Diverse physiology relies on receptor and transporter protein down-regulation mediated by ESCRTs. Mutations in ESCRT genes are thought to block this process, underlying pathogenesis of human cancers and neurological disorders. However, when orthologous mutations are introduced into model organisms, cells thrive and surface protein down-regulation persists, suggesting other mechanisms compensate for missing ESCRT activity. To better understand this secondary process, we studied degradation of quintessential ESCRT-client proteins (transporter Mup1, receptor Ste3) when ESCRT genes (VPS27, VPS36) are deleted in *Saccharomyces cerevisiae* using live-cell imaging and organelle biochemistry. We find that signaling for endocytosis remains intact, but all proteins aberrantly accumulate on vacuolar lysosome membranes in mutants and some wild type cells. Here they are sorted for degradation by the intralumenal fragment (ILF) pathway, either constitutively or when triggered by substrates, misfolding or TOR activation in vivo and in vitro. Thus, the ILF pathway functions as fail–safe layer of defense when ESCRTs disregard their clients, representing a two-tiered system that ensures down-regulation of surface polytopic proteins.

Author Contributions

Tom Kazmirchuck conducted experiments in figure 2.2

Tom Kazmirchuck conducted death assay in figure 2.3

Erin McNally conducted the experiments in figure 2.4

Erin McNally contributed videos and micrographs to figures 2.3, and 2.5

Acknowledgements

I would like to thank my supervisors Dr. Christopher Brett and Dr. Alisa Piekny for giving me the opportunity to take on this project. It was an immense privilege to learn from you both. I would like to especially thank Dr. Brett for his patience, guidance and encouragement throughout my studies.

I would also like to thank my committee members Dr. Malcolm Whiteway, and Dr. Laurent Potvin-Trottier for their insightful feedback and guidance.

Thank you to all current and former Brett lab members for your contribution and support.

Additionally, I would like to thank the *NSERC CREATE* Synthetic Biology Applications program for the exceptional training and support they provided me with throughout my degree.

Table of contents

List of Figures

List of Tables

List Of Abbreviations

AAA: ATPases associated with diverse cellular activities
ABC: ATP-binding cassette
AMP: adenosine monophoshate
ART: arrestin related family
ATP: adenosine triphosphate
AUX1: auxin transporter protein 1
CFTR: cystic fibrosis transmembrane conductance regulator
CHMP: charged multivesicular body protein
CHX: cycloheximide
CIC5: chloride/proton exchanger 5
CORVET: class C core vacuole/endosome tethering
CPS: carbamoyl phosphate synthetase
CPY : carboxypeptidase Y
CTL: control
Cx43: gap-junction connexin protein 43
CXCR: C-X-C chemokine receptor type 4
DIC: differential interference contrast
DNA: deoxyribonucleic acid
Dub: deubiquitylase
E1: ubiquitin activating enzyme
E2: ubiquitin conjugating enzyme
E3: ubiquitin ligase
EDTA: ethylenediaminetetraacetic acid
EGFR: epidermal growth factor receptor
EMCCD: electron multiplying charge coupled device
ENaC: epithelial sodium channel
ER: endoplasmic reticulum
ERAD: endoplasmic reticulum associated degradation
ESCRT: endosomal sorting complex required for transport
FET5: ferrous transport 5
FI: fluorescence intensity
FRAP: fluorescence retained after photobleaching
FTD: frontotemporal dementia
FYVE: phenylalanine-tyrosine-valine-glutamate
G6PDH: glucose-6-phosphate dehydrogenase
GDI: guanosine dissociation inhibitors
GFP: green fluorescent protein
GLUE: gram like ubiquitin EAP45

GLUT4: Glucose transporter type 4
GPCR: G-protein coupled receptor
GTP: guanosine-5'-triphosphate
HECT: homologous to the E6-AP carboxyl terminus
HEPES: 4-(2-hydroxyethyl)-1-piperazineethanesulfonic acid
HILO: highly inclined and laminated optical sheet
HOPS: homotypic fusion and protein sorting
HS: heat stress
HSC82: heat stress chaperone 82
HSP70: heat stress protein 70
ILF: intralumenal fragment
ILV: intralumenal vesicle
KCa3.1: intermediate-conductance Ca^{2+}-activated K^{+} channel
LAT: L-type amino acid Transporter
MAP: mitogen activated protein
MB: methylene blue
MHC: major histocompatibility complex
MVB: multivesicular body
NA: numerical aperture
Nav: voltage gated sodium channel
NEDD4: neuronal precursor cell-expressed developmentally downregulated 4
NPC1: Niemann Pick C1 protein
NPR1: nitrogen permease reactivator protein
NZF: Npl4 zinc finger
PAR1: protease activated receptor 1
PCR: polymerase chain reaction
PEST: rich in proline, glutamate, serine, and tyrosine
PI3P: phosphatidylinositol 3-phosphate
PIN: pin-formed protein (in plants)
PM: plasma membrane
PN: proteostasis network
PS: Pipe's sorbitol buffer
PY: P-P-X-Y-X-X-φ-φ, where P is a proline, Y a tyrosine, X any amino acid, and φ a hydrophobic amino acid
RBR: ring between ring finger
RING: really interesting new gene
RNA: ribonucleic acid
ROS: reactive oxygen species
SC: synthetic complete
sCMOS: scientific complementary metal–oxide–semiconductor

SDS: sodium dodecyl sulfate
SH3: SRC homology 3 domain
SNARE: SNAP receptor
SNF7: sucrose nonfermenting protein 7
SSA2: stress-seventy subfamily A protein 2
STAM: signal transducing adapter molecule
SUMO: small ubiquitin-like modifier
TFEB: transcription factor EB
TIRF: total internal reflection microscopy
TOR: target of rapamycin
TORC: target of rapamycin complex
UB: ubiquitin
UPR: unfolded protein response
UPS: ubiquitin proteosome system
VHS : protein domain occuring in Vps27, Hrs, and STAM
VM: vacuole membrane
VPS: vacuolar protein sorting
VRED: vacuole membrane protein recycling and degradation
WT: wild type
WW: typtophan-tryptophan
YPD: yeast extract peptone dextrose
ZNT1: zinc transporter 1

Chapter 1

Introduction

1.1 Proteostasis and protein degradation

In order to satisfy the conditions for essentially every cellular metabolic process, proteins must be synthesized, modified, delivered, and removed when they are no longer needed (*Pal & Eisenberg 2005; Hergyi & Gerstein 1999*). Synthesis is initiated when transcription factors activate the gene of interest, prompting its transcription into mRNA and export from the nucleus to the rough endoplasmic reticulum. There, proteins undergo translation, and proper folding into their tertiary conformations at the endoplasmic reticulum (ER). This biogenic process is costly to the cell, as it is no trivial task when considering, for example, the inter- and intra-molecular forces between the protein's constituents and the environment. This is why it is critical for the ER to have multiple quality control checkpoints, *e.g.,* Chaperone mediated protein folding (*Bukau et al. 2006; Wang et al. 2006)* and the Unfolded Protein Response (UPR) (*Ron & Walter 2007; Ruggiano et al., 2014)*. Once quality control checkpoints have been passed, proteins are exported in vesicles to the Golgi Apparatus, where they undergo maturation via glycosylation, sulfonation and phosphorylation and are ultimately packaged into either transport or secretory vesicles for delivery to their resident compartments or exportation from the cell (*Kurakawa & Nakano 2019; Matsuura-Tokita et al. 2006; Rothman & Wieland 1996*). These processes are dynamic in nature to ensure that overall cell function proceeds continuously and uninterrupted. The flux of all proteins in the cell is referred to as proteostasis; the pathways that orchestrate this turnover are referred to collectively as the proteostasis network (*Savitski et al. 2018; Hipp et al. 2019*). In humans, this network comprises over 2000 proteins highlighting that the cell has gone to great lengths to evolve a number of mechanisms to ensure the smooth flow of proteome turnover.

All proteins – soluble or polytopic – have finite lifetimes. This is because proteins succumb to damage, cleavage or misfolding over time due to ROS, heavy metals, toxins, and other stressors (*Lee et al. 2000; Salas-Moreno et al. 2019; Shivapurkar et al. 1987*). Even some of the longest lived, such as synaptic proteins, only have half-lives of 2-5 days (*Cohen et al. 2013*). Expired proteins must be selectively degraded to prevent aggregation and proteotoxicity, which are associated with numerous disorders and aging (*Reviewed by Balch et al., 2008; Calamini & Morimotoi, 2012; McLendon and Robbins, 2015; Höhfeld and Hoppe, 2018; Pataer et al. 2020*). Furthermore, downregulating their levels in response to substrates or cellular signaling is critical for proteostasis and underlies diverse physiology (*Roth et al. 1998*; *Babst, 2014; Hu & Sun, 2016; Cohen & Ziv, 2017; Hetz & Saxena, 2017*). Both quality control and triggered downregulation require discrete, selective removal of some individual proteins to

maintain or remodel the landscapes of compartmental membranes; and to preserve or modify cell compartment integrity, identity and function without complete replacement of the organelle.

1.2 Proteotoxicity and disease

When the integrity of the proteostasis network is threatened, the cell's ability to adequately manage the burden of protein turnover is impeded, leading to accumulation of misfolded, un-needed or unfunctional protein, and imbalances in nutrient pools (*Abu-Remaileh et al. 2017*). Dysfunctions in the proteostasis network occur because of mutations or environmental damage, which accumulate with age (*David et al. 2010; Taylor & Dillin 2011*) and underlie diverse pathophysiology– including neurodegenerative (*Komatsu et al. 2006; Lin et al. 2015*), metabolic (*Reviewed by Platt et al. 2018; Aerts et al. 2019*), and cardiac diseases (*Zhang et al. 2014; Dai et al. 2008*), as well as cancer (*Xu et al. 2009; Liu et al. 2018)* e.g. In humans, loss of function mutations to the gene encoding cystinosin (CTNS), a lysosomal membrane transporter that exports cysteine to the cytosol, leads to excessive buildup of cysteine in lysosomes, affecting all tissues but having especially pronounced effects on kidney function*)*, growth, vision and thyroid function *(Reviewed by Elmonem et al. 2016*). Conversely, gain-of-function mutations that perturb protein flux can pose significant threats to cell integrity e.g. In mammals, gain-of-function mutations to the epidermal growth factor receptor (EGFR) can render this protein insensitive to downregulation, causing aberrant activation of signalling pathways, resulting in uncontrolled growth, proliferation pathways, and often leading to cancer (*Zhang et al. 2013; Reviewed by Sigismund et al. 2018*).

1.3 Polytopic Protein Downregulation

Polytopic proteins (also called integral or membrane proteins) are paramount for proper cell physiology, accounting for over 30% of the human proteome (*Fagerberg et al. 2010*; *Dobson et al. 2015*) and comprise an important part of the proteostasis network (*Labbadia & Morimoto 2015; Hegde & Zavodszky 2019*). Of particular interest are surface polytopic proteins, as they are involved in a plethora of essential functions that collectively confer cellular identity and physiological state of the cell (*e.g.* selective MHC-II expression on the plasma membrane of macrophages, dendritic cells, B-cells and the epithelial cells of the lung and intestine; *Hewitt 2003; ten Broeke et al. 2013; Wosen et al. 2018*), and are crucial for cell-cell communication (*Latif et al. 2005*), nutrient absorption (*Asaoka et al. 2016; Keller et al. 1989*), neurotransmitter uptake (*Miledi et al. 2002*) and environmental adaptation (*Liu et al. 2018*). When surface polytopic proteins misfold, become damaged, or no longer needed, they are labeled for downregulation and are transported to the lysosome for degradation.

Lysosomes, the recycling units of the cell and an essential component of the proteostasis network, are conserved in eukaryotes. In yeast, they appear as large membrane bound

compartments called vacuoles (*Reviewed by Li et al. 2009*), whereas mammalian lysosomes are more heterogenous in structure (*Reviewed by Ballabio 2016*). These dynamic organelles undergo continuous cycles of homotypic fusion and fission in order to regulate their numbers, ensure organellar inheritance, and maintain protein and lipid homeostasis (*Luzio, Pryor & Bright 2007; Wickner & Haas 2000; McNally, Mahmoud, Brett 2017; Castellano et al. 2017*). They were first observed 70 years ago, when de Dube and colleagues found membrane enclosed organelles containing hydrolytic enzymes (*Dubé et al. 1955*). The following year, Novikoff observed similar organelles that contained cellular contents using electron microscopy of rat liver cells (*Novikoff, Beaufay & de Dube 1956)*. These two findings led to the discovery of specialized cellular compartments dedicated to the degradation of biomolecules. Today, lysosomes are recognized as the terminal points for endocytosis and autophagy and are responsible for the downregulation of nearly all membrane bound proteins (*Settembre et al. 2013; Luzio et al. 2014*).

1.4 The MVB pathway

In the early 2000s it was observed using *S. cerevisiae* that selective downregulation of certain surface polytopic proteins to the lysosome was dependent on the endosomal sorting complexes required for transport (ESCRT) (*Katzmann et al. 2001; Babst et al. 2002a; Babst et al. 2002b; Babst et al. 1997*). Of the five ESCRTs, ESCRT-0, -I and –II recognize ubiquitin patterns on client proteins and sort them into patches of the endosome membrane that bud inwards towards the lumen where ESCRT-III recruits cargo into these furrows (*Hurley, 2010; Ren & Hurley 2010*). To complete the process, Vps4 an AAA-ATPase which comprises of the membrane fission machinery, pinches the neck of the forming vesicle to release it into the endosome lumen (*Adell et al., 2014; Yang & Hurley 2010*). This process occurs repeatedly along the limiting membrane of the endosome until maturation into a multivesicular body (MVB), which contains many ILVs coated with client protein (*Reviewed by Babst 2011*). Upon heterotypic fusion of the MVB to the lysosome, the ILVs are delivered to the lysosomal lumen and degraded by acid hydrolases into amino acids. These metabolites are recycled back to the cytosol to replenish amino acid levels (*Abu-Remaileh et al. 2017*). Collectively, this process is termed the MVB pathway.

The MVB pathway is widely regarded to be the only pathway that accounts for selective downregulation of all surface protein. While there is no doubt that the MVB pathway plays an important role in cell proteostasis, evidence is emerging that other pathways may be involved selectively downregulating polytopic proteins: While the MVB pathway has been shown to mediate delivery of many proteins, reports of ESCRT non-canonical or independent pathways for protein downregulation in yeasts, plants, and mammals have been emerging (*McNally & Brett 2018; Lee et al. 2017; Parkinson et al. 2015; Bowers et al. 2006; Theos et al. 2006;*

Silverman et al. 2013; Leung et al. 2008). Additionally, extensive research into these complexes has revealed that they play a myriad of physiologically relevant cellular roles, e.g., regulation of cytokinesis, exosome biogenesis and viral budding (*Reviewed by Vietri et al. 2019*), suggesting that sorting into the MVB pathway may in fact be a specialized function of these complexes. Importantly, ESCRT mutations are not lethal, but are implicated in several neurodegenerative diseases, including frontotemporal dementia (FTD) (*Filimonenko et al. 2007; Reviewed by Rusten & Simonsen 2008*), strongly suggesting that alternative pathways may compensate or work in concert with the MVB pathway to coordinate selective polytopic protein downregulation in diverse cell types. Importantly, around the time when ESCRTs were discovered, it was independently observed that the membranes of each vacuole form a vertex ring made up of fusogenic lipids and proteins where their membranes overlap, termed the boundary membrane, which can be internalized upon homotypic fusion, producing an intralumenal fragment within the lumen of the fused vacuole (*Wickner & Haas 2000; Wang et al. 2002; Fratti et al. 2004; Mattie et al. 2017*). This prompted investigation into whether this fragment could be of physiological relevance and led to the discovery of the IntraLumenal Fragment (ILF) pathway, a lysosomal degradation pathway that selectively downregulates lysosome and plasma membrane resident proteins.

1.5 The ILF Pathway

Until recently, it was unclear how resident polytopic proteins embedded within lysosome membranes were selectively degraded. These proteins are particularly susceptible to cleavage from lumenal proteases and to damage from reactive oxygen species generated from lumenal iron stores, despite protection offered by the glycocalyx lining the lumenal face of the membrane (*Kosicek et al. 2018*). They must be replaced to maintain function and prevent accumulation that leads to lysosomal membrane permeability or rupture causing cell death. These include nutrient transporters critical for biomaterial recycling, including those that maintain free amino acid pools needed for protein biogenesis and proteostasis (*Abriel et al 2005*). Thus, selective clearance of only damaged or unneeded proteins is important for organelle maintenance and integrity as well as functional remodeling for cell metabolism.

Lysosomes must undergo membrane fusion with autophagosomes or MVBs to receive biomaterials for recycling, a critical aspect of these lysosome degradation pathways. But lysosomes also fuse with themselves (and undergo fission) for compartmental remodeling – form large vacuoles or reticular networks, for maintenance of numbers, and for organelle inheritance (*Luzio, Pryor & Bright 2007; Wickner & Haas 2000; McNally, Mahmoud, Brett 2017; Castellano et al. 2017*). Based on the observation that lysosomal vacuoles internalize a portion of their membranes upon homotypic fusion in the model organism *Saccharomyces cerevisiae* (*Wang et al., 2002*), we discovered that resident transporter proteins were selectively degraded during this process (*McNally et al., 2017*): Upon misfolding, cellular signaling or changes in

substrate levels, vacuole membrane proteins are selectively sorted into an area of membrane that forms the boundary or interface between docked organelles. This "boundary" membrane is encircled by a ring of fusogenic lipids and proteins that bridge closely apposed organelles (*Wang et al., 2003; Fratti et al., 2014*). Upon lipid bilayer merger at this ring, the protein-laden boundary membranes are internalized as an intralumenal fragment (ILF) and degraded by lumenal hydrolases (see *Mattie et al., 2017; Karim et al., 2018*). Importantly, systematic deletion of genes encoding components of ESCRTs or the autophagy machinery had no effect on this process, confirming that it is a third independent lysosome degradation pathway.

Although unique in many respects, all three pathways must include the same four consecutive stages to function: protein labeling, sorting, internalization and degradation. For the ILF pathway, much of the underlying molecular machinery remains enigmatic but preliminary work suggests the following:

Labeling. This remains unclear, but client proteins studied have been shown to be ubiquitylated under conditions that stimulate degradation, based on proteomic analysis (*Rayner et al. 2019*). Adapter proteins and E3-ligases can be recruited to vacuole membranes (*Zhu et al. 2017*), and the ILF pathway supposedly shares client proteins with ESCRTs (e.g. the stalk domain of the V-type H^+-ATPase Vph1; *McNally et al. 2017*) also raising the possibly that protein ubiquitylation may be involved.

Sorting. Although the exact mechanism of client protein recognition remains elusive, it is clear that that some resident polytopic proteins are depleted whereas others are enriched within boundary membranes (*McNally et al 2017; McNally & Brett 2018).* Lateral movement of these membrane proteins into or out of this region, seems to occur during formation of this interface, based on FRAP experiments targeting this microdomain (*McNally et al. 2017*). Many protein complexes form an assembly at the vertex ring encircling this boundary area (*Wickner & Haas 2000*), possibly contributing to client protein sorting. When activated, the Rab-GTPase Ypt7 is thought to drive this process (*Haas et al. 1995*), Bypassing the requirement for Rab-GTPase component of the fusion machinery (*Mattie et al. 2017*), suggesting that components of this assembly like contribute to client protein sorting. It may both sort and internalize similar to assembly of ESCRTs at the site of ILV formation.

Internalization. Unlike ESCRT-mediated pathways reliant on membrane fission, the ILF pathway relies on membrane fusion to merge boundary membranes that creates a relatively large protein-laden intralumenal vesicle. Because fusion is a requisite of organelle homeostasis and function, it offers an auto housekeeping function. a new way of making membrane vesicles reliant on fusion instead of fission and excludes ESCRTs, raising the possibility that it also mediates ILVs observed in the past (*e.g.* ESCRT independent biosynthesis of mammalian ILVs; *Stuffers et al. 2009*). Notably, homotypic vacuole fusion does not require ILF formation (i.e.

some fusion events do not produce ILFs; *Mattie et al., 2017; Karim et al., 2018*), suggesting that the protein internalization stage can be regulated to optimize membrane protein degradation.

***Degradation*.** within the vacuole lumen the polypeptides and lipids that compose the ILF are catabolized by acid hydrolases – the terminal stage shared by all lysosomal degradation pathways.

1.6 Triggers

The ILF pathway mediates the degradation of client proteins in response to diverse stimuli. Importantly, the ILF pathway has recently been shown to mediate downregulation of several surface proteins to the lysosome for degradation (*McNally & Brett 2018*). ILF client protein are downregulated in response constitutive turnover, peripheral quality control, presence of substrate or ligand, and cell signalling:

Constitutive. Lysosomes are important stores for bioactive metals, including cadmium, iron and zinc, needed for activity of many cellular enzymes including lumenal metalloproteases (*Marigomez et al. 1989; Li & Kaplan 1998; Roh et al. 2012*). The iron permease Fth1 (*Urbanowski & Piper, 1999*) is a client of the ILF pathway (*McNally et al., 2017*). ZNT1, a protein involved in divalent cation transport through the vacuole membrane,) is involved in calcium, zinc, and neurotransmitter homeostasis. Its yeast ortholog Cot1, is constitutively turned over by the ILF pathway (*McNally et al. 2017*). Lumenal iron and zinc homeostasis must be carefully controlled when cells are challenged with oxidative stress to prevent generation of reactive oxygen species (*Galaris et al. 2019; Rajapakse et al. 2017*). ROS damages vacuole membranes, leading to rupture, release of lumenal hydrolases into the cytoplasm and cell death – a process called lysosomal cell death (*Kroemer & Levine 2008*). Ycf1, an ATP-binding cassette (ABC) transporter for glutathione, that has been shown to be important for lysosomal homeostasis fusion, is also an ILF client (*Sasser et al. 2013*). Glutathione is an important antioxidant that is primarily stored in lysosomes/vacuoles (*Homma & Fujii 2015*). Thus, the ILF pathway may control Fth1, Cot1 and Ycf1 protein levels when cells are under oxidative stress to prevent vacuole membrane damage and lysosomal cell death.

Peripheral quality control. Thus far, we have identified 10 resident vacuole membrane proteins that selectively degraded by the ILF pathway in *Saccharomyces cerevisiae*; all of which have human orthologs found on lysosomes. This includes the stalk domain of the V-type H^+-ATPase Vph1, which maintains the acidic lumenal environment essential for lysosome physiology (*Manolson et al. 1992*), as well as two amino acid transporters (Vba4 and Ypq1) and the sterol transporter Ncr1, the yeast ortholog of human NPC1, which are critical for proteostasis and lipid metabolism (*Winkler et al. 2019*). Ybt1, An ATP-dependent bile permease, is a member of the ABC transporter superfamily. Importantly, Ybt1 mediates transport of phosphatidylcholine to

the vacuole lumen. It is also involved in the negative regulation of vacuole fusion (*Sasser et al. 2012*). Progressive loss of the vacuole/lysosome pH gradient and changes in lipid and protein metabolism are implicated in chronological and replicative cellular aging programs (*Bahr & Bendiske 2002; Carmona-Gutierrez 2016*). Thus, by controlling Vph1, Vba4, Ypq1, Ncr1, and Ybt1 protein levels, the ILF pathway may be important for remodeling the lysosome membrane protein landscape to mediate changes in metabolism that are critical for survival when cells are starved or when they age.

Substrates/ligands. In *Saccharomyces,* the low affinity hexose transporter Hxt3 plays an important role in responding to changes in the extracellular environment, specifically in response to certain glucose concentrations (*Roberts & Hudson 2006*). Hxt3 is expressed on the plasma membrane when extracellular glucose levels are abundant. It is rapidly downregulated upon glucose starvation and sent to the vacuole lumen for degradation. Instead of being packaged into intralumenal vesicles by ESCRT machinery, Hxt3 accumulates on the limiting membrane of the endosome, which upon heterotypic fusion, delivers the protein to the membrane of the vacuole (*McNally & Brett, 2018*). Hxt3 is then selectively sorted to the boundary membrane of the vacuole and upon homotypic vacuole fusion is internalized bound to an intralumenal fragment. Notably, GLUT4, a human ortholog of Hxt3, is also expressed when extracellular glucose levels are abundant and rapidly downregulated when glucose levels are low, however, to date the precise mechanism is still not fully understood (*Chen et al. 2015*). Some other surface protein clients include: Itr1, A myo-inositol transporter part of the sugar transporter superfamily (*McNally & Brett 2018*). Aqr1, a uniporter that confers resistance to short chain monocarboxylic acids and quinine in yeast and is implicated in the secretion of homoserine and threonine (*Velasco et al. 2004*).

***Cell Signalling*.** Downregulation of ILF client proteins is also induced by cycloheximide, a fungicide that inhibits protein translation in eukaryotes by binding to the E region of the ribosome, blocking amino acid addition onto growing polypeptide chains (*Cooper & Bossinger, 1976*; *Roth & Dampier, 1972*). Cycloheximide is also an activator of the Target of Rapamycin Complex or TORC1/2. TORC is a conserved, critical sensor of nutrient levels in the cell and regulator of growth and proliferation. Although the precise interaction between CHX and TORC is not fully understood, one hypothesis is that cycloheximide activates TOR signaling indirectly due to its inhibitory effects on translation, thereby increasing the cytosolic concentration of free amino acids and activating TOR signaling (*Beugnet et al 2003*). For a more in-depth summary of TOR signaling and its physiological implications in Saccharomyces, refer to the following review (*Loewith & Hall 2011*).

1.7 How do the ILF and MVB pathways coordinate in S. cerevisiae?

It remains unclear how the ILF pathway coordinates with ESCRTs to mediate surface protein down-regulation: Are MVB client protein still degraded when ESCRTs are impaired? If so, are these client proteins instead delivered to the vacuole by the ILF pathway? Under what conditions does this occur (*i.e., in response to constitutive turnover, peripheral quality control, substrate, or cell signalling*)? Do these two pathways share client proteins?

To answer these questions, I used the model organism *S. cerevisiae* to study surface protein downregulation. *S. cerevisiae* provides several significant advantages over mammalian models as a model organism to study the molecular underpinnings of the lysosomal degradation pathways: While *S. cerevisiae* generally have 2 – 5 large (400 – 1,500 nm diameter) vacuoles per cell, mammalian cells each contain between 50 – 1,000 small (100 – 300 nm diameter) lysosomes, whose structure and function are thought to be very heterogeneous, making them difficult to study using light microscopy and biochemical methods (*Ballabio A. & Bonifacino J.,S., 2020*); Secondly, ease of growth accommodates large quantities necessary for detailed biochemical analysis, with short doubling times (1.5 hours) permitting high experimental turnover at a fraction of the time it takes when using mammalian models (*Olivares-Marin et al. 2018*) Adding to that is cost effectiveness, as growth reagents are abundant and inexpensive facilitating experimental exploration, upscaling and drug discovery (*Du et al. 2019; Monti et al. 2019*); Furthermore, their vacuole membranes can be easily visualized using the lipophilic dye FM4-64 by fluorescence microscopy, permitting observation of organelle dynamics and changes in membrane protein distribution in near real–time (*Vida & Emr 1995*); its genetic toolkit is unmatched permitting advanced, complementary genetic analysis, e.g. genomic knockout or knock-in (*Franzmann et al. 2018; Monti et al. 2019*) and its genome was the first eukaryotic one to be sequenced (*Bassett et al. 1996; Dujon et al. 2004*), with libraries of hundreds of thousands of strains available, representing comprehensive sets of genomic modifications, e.g. GFP knocked in behind every genes, every (viable) gene knocked out (*Giaever et al. 2002; Huh et al. 2003; Tarassov et al. 2008; Yofe et al. 2016*).

My research primarily focused on the downregulation of two polytopic proteins: The high affinity methionine permease, Mup1 who, along with its paralog Mup3, are the only transporters in *S. cerevisiae* that are members of the L-type amino acid transporters (LAT) a physiologically important family of transporters and potential therapeutic target for cancer treatment in humans (*reviewed by Häfliger & Charles 2019*); and the mating pheromone, Ste3 a yeast GPCR (*Bassett et al. 1996).* Importantly, both of these proteins had previously been demonstrated to be downregulated by the MVB pathway in response to constitutive regulation, presence of ligand or substrate, in response to protein misfolding (*e.g.,* by experimentally

subjected cells to heat stress), and in response to TOR signalling (*Guiney et al. 2016; Shields et al. 2009*).

I systematically subjected strains with GFP-tagged proteins to different stimuli in order to trigger surface protein downregulation. I then assessed whether these proteins were still being degraded in ESCRT mutants (vps27Δ and vps36Δ; bridging components of ESCRT-0 and -II, respectively) by western blot analysis. I also followed the cellular route taken by these proteins during downregulation from the plasma membrane to the vacuole using fluorescence microscopy. Remarkably, Mup1-GFP vps27/36Δ and Ste3-GFP vps27Δ are sorted into the ILF pathway for lysosomal degradation when ESCRTs are impaired in response to diverse stimuli. This finding not only suggests that the ILF pathway plays an important compensatory role when ESCRTs malfunction, but also that there exists a degree of overlap between these two pathways, as both are capable of recognizing these surface proteins.

The constitutive turnover of both Mup1 and Ste3 results in high lumenal vacuole GFP signal in both wild-type and vps27/36Δ strains. This can make visualizing GFP localization to vacuole membrane technically challenging. I therefore took advantage of the pH sensitive GFP variant pHluorin, whose signal is quenched when exposed to the acidic lumen of the vacuole (pH ~ 5.0), to obtain better resolution of client protein localization to the boundary membrane, a hallmark of the ILF pathway. Remarkedly, both Mup1 and Ste3 are sorted to the boundary membrane and internalized as an ILF in vps27/36Δ strains in response to diverse stimuli.

Lastly, to assess whether ILF and MVB pathways share clients, I used pHluorin tagged strain to assess whether either protein localized to the vacuole membrane when ESCRTs were functioning. Surprisingly, Ste3-pH is downregulated by the ILF pathway constitutively and in response to heat stress, suggesting that Ste3 is a shared client protein of the ESCRT and ILF pathways. While the ILF pathway delivered Mup1-pH vps27/36Δ strains to the vacuole, there was no appreciable detection of GFP signal on the vacuole or boundary membranes in wild-type Mup1-pH, suggesting that Mup1 is preferentially an MVB client protein. Therefore, the ILF pathway seems to represent a secondary lysosomal degradation route that depends on the fusion machinery of the vacuole to degrade MVB client proteins when the ESCRTs are impaired. Furthermore, the ILF pathway represents a means for regulating levels of Ste3, pointing to its important role in coordinating with the MVB pathway to ensure proper transmembrane proteome turnover, even when the former is intact.

1.8 Summary

To summarize, the ILF pathway coordinates with the MVB pathway to function as a two-tiered system for the downregulation of polytopic surface transporters and receptors to the lysosome. Given that there have been previous reports of ESCRT-independent downregulation

of proteins in fungi, plants, and humans (*McNally & Brett 2018; Lee et al. 2017; Parkinson et al. 2015; Bowers et al. 2006; Theos et al. 2006; Silverman et al. 2013; Leung et al. 2008*), and that the ILF pathway is dependent on fusion machinery of the lysosome (a conserved feature of this organelle) it is likely conserved in eukaryotes. Furthermore, improper protein turnover is a crucial catalyst in diverse pathophysiology, thus, these findings provide an exciting avenue for the development of potential novel therapeutics (*e.g.,* by upregulating the rates of homotypic fusion) and is a current focus of investigation. Future work will also focus on uncovering the molecular switches that allow proteins to enter the ILF pathway, as well as establish whether any exclusion from the exists (e.g are all MVB clients potential ILF clients?).

Chapter 2

Manuscript: A Two-Tiered System for Surface Receptor and Transporter Protein Down-Regulation

2.1 Foreward

In this study, we investigated whether surface transporters and receptors were regulated by the ILF pathway, as we had previously shown the low affinity glucose transporter, Hxt3 to be exclusively downregulated by this mechanism (McNally & Brett 2019).

2.2 Introduction

Precise control of surface receptor, transporter and channel protein lifetimes underlies diverse physiology, including immune responses, endocrine function, tissue development, nutrient absorption, metabolism and synaptic plasticity (*Katzmann et al., 2002; Palacios et al., 2005; Rodahl et al., 2008; Lobert et al., 2010*; *Zhou et al., 2010; Hislop and von Zastrow, 2011*; *Koumanov et al., 2012; Chassefeyre et al., 2015*). Damaged surface proteins must also be cleared from the plasma membrane to prevent proteotoxicity (*Wang et al., 2011; Keener and Babst, 2013; Zhao et al., 2013*). These damaged or unneeded polytopic proteins are first labeled and selectively internalized within the cell by endocytosis (*Blondel et al., 2004; Lewis and Pelham, 2009; MacGurn et al., 2011; Jones et al., 2012; MacDonald et al., 2012; Keener and Babst, 2013; Babst, 2014*). At endosomes, these proteins are packaged into intralumenal vesicles (ILVs) by ESCRTs (Endosomal Sorting Complexes Required for Transport) (*Henne et al., 2011*). Many rounds of ILV biogenesis forms a multivesicular body (MVB) (*Nickerson et al., 2010; Hanson and Cashikar, 2012*). Once mature, the perimeter membrane of the MVB fuses with the lysosome membrane, exposing protein-laden ILVs to lumenal acid hydrolases for degradation (*Katzmann et al., 2002; Karim et al., 2018a*).

Although this ESCRT-dependent MVB pathway is clearly important for proteostasis, reports of ESCRT-independent down-regulation have emerged (*Bowers et al., 2006; Theos et al., 2006; Leung et al., 2008; Babst, 2011; Silverman et al., 2013; Parkinson et al., 2015*). These observations challenged the presumption that this fundamental process is exclusive, which led to our recent discovery of an alternative called the ILF pathway (*McNally et al., 2017; McNally & Brett, 2018*): In the model organism *S. cerevisiae*, we found that some surface transporter proteins bypass ESCRTs on endosomal membranes after endocytosis, and thus remain on perimeter membranes of mature MVBs. Upon subsequent fusion with vacuolar lysosomes (or vacuoles), these transporters are deposited onto vacuole membranes. Here, they are sorted into a disc encircled by a ring of fusogenic lipid and

proteins that forms at the vertex between two docked organelles (*Wang et al., 2003; Fratti et al., 2004*). Upon homotypic vacuole membrane fusion at this vertex ring, apposing protein-laden discs merge, forming an intralumenal fragment (ILF) that is exposed to lumenal hydrolases and catabolized (*Wang et al., 2002; Mattie et al., 2017; Karim et al., 2018b*).

Protein degradation by the ESCRT-independent ILF pathway or canonical MVB pathway are triggered by similar stimuli, such as protein misfolding by heat stress for quality control, TOR signaling, or changes in substrate levels (*MacGurn et al., 2011; Jones et al., 2012; Keener & Babst, 2013; Babst, 2014; McNally et al., 2017; McNally & Brett, 2018*). This suggests they play comparable roles in regulating surface protein lifetimes for proteostasis and physiology. However, the basis of pathway selection by client proteins remains obscure, and it is unclear whether these pathways can share client proteins. This is important because some human cancers and neurological disorders are linked to loss-of-function mutations in genes encoding ESCRT subunits that presumably block the MVB pathway (*Saksena & Emr, 2009*). Deleting these genes in model organisms has implicated persistence of residual ESCRT-client protein catabolism (*Trajkovic et al., 2008; Blanc et al., 2009; Stuffers et al., 2009b; Edgar et al., 2014*), suggesting that another mechanism is compensating for their loss. Herein, we test the hypothesis that the ILF pathway down-regulates these ESCRT-client proteins when they are not recognized by the canonical MVB pathway.

2.3 Methods

2.3.1 Yeast strains and reagents

Saccharomyces cerevisiae strains used in this study are listed in **Table 2.1.** Mat-α yeast deletion clones used are from the complete set purchased from Invitrogen Corp. (Cat# 95401.H2; Carlsbad, USA). Strains generated for this study are available from the corresponding author upon reasonable request. We knocked out VPS27 or VPS36 by homologous recombination using the Longtine method (*Longtine et al., 1998*) and primer sets described previously (*McNally & Brett, 2018*). Genomic mutations were confirmed by sequencing. GFP or pHluorin genes were integrated into the genome behind genes of interest to ensure minimal effects on native gene expression. All reagents for molecular biology (enzymes, polymerases, ligases) were purchased from New England Biolabs (Ipswich, USA). Biochemical and yeast growth reagents were purchased from Sigma-Aldrich (Oakville, Canada), Thermo-Fisher Scientific (Burlington, Canada), or BioShop Canada Inc (Burlington, Canada). Recombinant rabbit IgG raised against GFP (B2) or Pho8 (1D3A10) were purchased from Abcam (Cat# ab290, Cat# ab113688; Toronto, Canada) and rabbit IgG against G6PDH was purchased Sigma-Aldrich (Cat# A9521).

Horseradish peroxidase-labeled affinity purified IgG to rabbit was purchased from SeraCare (Cat# 5450-0010; Milford, USA). Recombinant Gdi1 protein was purified from *E. coli* cells using a calmodulin-binding peptide intein fusion method (*Brett & Merz, 2008*). Recombinant Gyp1-46 protein (representing the catalytic domain of Gyp1, a Rab-GTPase activating protein) was purified as previously described (*Eitzen et al., 2000*). Reagents used in vacuole fusion reactions were prepared in 20 mM Pipes-KOH, pH 6.8, and 200 mM sorbitol (Pipes Sorbitol buffer, PS).

Table 2.1. *Saccharomyces cerevisiae* strains used in this study

Strain	Genotype	Source
SEY6210	*MATα, leu1-3, 112 ura3-52 his3-200, trp1-901 lys2-801suc2-D9*	*Robinson et al., 1988*
BY4741	*MATa his3-Δ1 leu2-Δ0 met15-Δ0 ura3-Δ0*	*Huh et al., 2003*
Fet5-GFP	BY4741, *Fet5-GFP::HIS3MX*	*Huh et al., 2003*
Fth1-GFP	BY4741, *Fth1-GFP::HIS3MX*	*Huh et al., 2003*
Fet5-GFP:: *vps36Δ*	BY4741, *Fet5-GFP::HIS3MX, vps36Δ:KanMX*	*McNally et al., 2017*
Mup1-GFP	SEY6210, *Mup1-GFP::KanMX*	*Prosser et al., 2010*
Mup1-GFP:*vps27Δ*	SEY6210, *Mup1-GFP::KanMX, vps27Δ:HIS3MX*	This study
Mup1-GFP:*vps36Δ*	SEY6210, *Mup1-GFP::KanMX, vps36Δ:HIS3MX*	This study
Mup1-pHluorin	SEY6210, *Mup1-pHluorin::KanMX*	*Prosser et al., 2010*
Mup1-pHluorin:*vps27Δ*	SEY6210, *Mup1-pHluorin::KanMX, vps27Δ:HIS3MX*	This study
Mup1-pHluorin:*vps36Δ*	SEY6210, *Mup1-pHluorin::KanMX, vps36Δ:HIS3MX*	This study
Ste3-GFP	SEY6210, *Ste3-GFP::KanMX*	*Prosser et al., 2010*
Ste3-pHluorin	SEY6210, *Ste3-pHluorin::KanMX*	*Prosser et al., 2010*
Ste3-GFP:*vps27Δ*	SEY6210, *Ste3-GFP::KanMX , vps27Δ:HIS3MX*	This study
***vps27*Δ**	BY4741, *vps27Δ:KanMX*	Invitrogen Corp.
***vps36*Δ**	BY4741, *vps36Δ:KanMX*	Invitrogen Corp.

***hsc82*Δ**	BY4741, *hsc82Δ:KanMX*	Invitrogen Corp.
***ssa2*Δ**	BY4741, *ssa2Δ:KanMX*	Invitrogen Corp.
***snf7*Δ**	BY4741, *snf7Δ:KanMX*	Invitrogen Corp.
***vps23*Δ**	BY4741, *vps23Δ:KanMX*	Invitrogen Corp.
***fet5*Δ**	BY4741, *fet5Δ:KanMX*	Invitrogen Corp.

2.3.2 Western blot analysis

For analysis of whole cell lysates, yeast cells were prepared as previously described (*Volland et al., 1994*). Cells were grown in culture to mid-log phase, washed once with YPD (yeast extract peptone dextrose) medium, resuspended in fresh YPD medium, and incubated at 30˚C in the presence or absence 100 μM cycloheximide for 120 minutes, or incubated at 42 ˚C for 30-60 minutes for heat stress. To trigger down-regulation of Mup1 by methionine, cells were instead grown in culture to mid-log phase in washed synthetic complete medium lacking methionine (SC –met), collected and washed once with SC –met, then resuspended in SC with 0.2 mM methionine and incubated at 30 ˚C for up to 30 minutes. After treatment, 5 OD_{600nm} units of cells were collected, resuspended in 0.5 mL of lysis buffer (0.2 M NaOH, 0.2 % β-mercaptoethanol) and incubated on ice for 10 minutes. Samples were then treated with trichloroacetic acid (5 % final concentration) and incubated on ice for an additional 10 minutes. Precipitates were collected by centrifugation (12,000 x g for 5 minutes at 4 ˚C) and resuspended in 35 μL of dissociation buffer (4 % SDS, 0.1 M Tris-HCl, pH 6.8, 4 mM EDTA, 20 % glycerol, 2 % β- mercaptoethanol and 0.02 % bromophenol blue). Samples were treated with Tris-HCl, pH 6.8 (0.3 M final concentration) and incubated at 37 °C for 10 minutes. For analysis of in vitro fusion reactions, samples were prepared from isolated vacuoles as previously described (*McNally et al., 2017*).

Whole cell lysates or isolated vacuole preparations were then loaded into 10 % SDS-polyacrylamide gels. After electrophoresis, separated proteins were transferred to nitrocellulose membranes and probed with antibodies raised against GFP (1:1,000), G6PDH (1:1,000) or Pho8 (1:1,000). For secondary labeling, blots membranes were stained with horseradish peroxidase- labeled affinity purified polyclonal antibodies to rabbit (1:10,000). Please refer to manufacturer's website for antibody validation. Chemiluminescence of stained membranes was digitally imaged using a GE Amersham Imager 600 (GE Health Care, Piscataway, USA). Blots shown are best representatives of 3 or 4 biological replicates, each repeated at least twice (technical replicates). Band density was measured using ImageJ software.

2.3.3 Live cell imaging

Live yeast cells were treated with FM4-64 to exclusively stain vacuole membranes as previously described (*Brett et al., 2008*). To stimulate down-regulation of pHluorin- or GFP-tagged surface proteins, cells in SC medium were treated with or without either 0.2 mM methionine for up to 30 minutes at 30 ˚C or 100 µM cycloheximide for 90 minutes at 30 ˚C, or incubated at 42 ˚C for 30 minutes for sublethal heat stress (see *McNally & Brett, 2018*). After treatments, cells were immediately placed between pre-warmed glass coverslips at 30 ˚C and imaging by HILO microscopy. For time-lapse videos, cells were plated on coverslips coated with concavalin-A (1mg/ml in 50 mM HEPES, pH 7.5, 20 mM calcium acetate, 1 mM $MnSO_4$) and imaged at 30 ˚C using a Chamlide TC-N incubator (Live Cell Instrument, Korea).

2.3.5 Highly inclined laminated optical sheet (HILO) microscopy

Cross sectional images were acquired 1 µm into the sample using a Nikon Eclipse TiE inverted microscope equipped with a TIRF (Total Internal Reflection Fluorescence) illumination unit, Photometrics Evolve 512 EMCCD (Electron Multiplying Charge Coupled Device) or Photometrics Prime BSI sCMOS (scientific complementary metal–oxide–semiconductor) camera, Nikon CFI ApoTIRF 1.49 NA 100 X objective lens, and 488 nm or 561 nm 50 mW lasers operated with Nikon Elements software (Nikon Instruments Inc., Mississauga, Canada). Micrographs or movies shown are best representatives of 2 – 12 biological replicates (each represents a sample prepared on different days from a separate yeast culture), imaged at least 8 times each (technical replicates) whereby each field of view examined contained > 30 cells or isolated organelles.

2.3.6 Cell viability assay

As previously described (*Karim et al., 2018b*), yeast cell cultures were grown in SC medium for 16 – 18 hours at 30 ˚C, sedimented, washed once with SC, resuspended in fresh SC, and incubated at either room temperature (control) or 50 ˚C (lethal heat stress) for 30 minutes. After incubation cells were washed once with fresh SC, resuspended in 100 µL SC and mixed with 100 µL 0.1 % (w/v) methylene blue stock solution (0.1 g dissolved in 100 mL dH_2O), and incubated for 5 minutes at room temperature. Images were acquired using a Nikon Eclipse TiE inverted epifluorescence microscope equipped with a Nikon DsRi2 color CMOS (complementary metal-oxide semiconductor) camera, Nikon CFI 40 X Plan Apo Lambda 0.95 NA objective lens and DIC optics (Nikon Instruments Inc.). Viable cells were colorless and dead cells were blue. Cells were counted using ImageJ software (National Institutes of Health, Bethesda, USA) semi-automated cell counter macro. Data are reported as mean ± S.E.M of the percentage of blue cells observed within the population. Micrographs shown are best representatives of 2 – 4 biological replicates (each a

single sample prepared from a separate yeast culture on different days), imaged at least 6 times each (technical replicates) whereby each field examined contained > 100 cells.

2.3.7 Vacuole isolation and homotypic vacuole fusion

Vacuoles were purified from yeast cells as previously described (*Haas et al., 1995*): Cells were harvested, washed, treated with oxalyticase to generate spheroplasts, and gently permeabilized using DEAE-dextran. Then vacuoles were isolated on a ficoll gradient by ultracentrifugation (100,000 x g, 90 minutes, 4 ˚C). Homotypic vacuole fusion reactions contained 6 µg of isolated vacuoles in standard fusion reaction buffer with 0.125 M KCl, 5 mM $MgCl_2$, and 10 µM CoA. 1 mM ATP was added to initiate fusion. Vacuolar membranes were stained with 3 µM FM4-64 for 10 minutes at 27 ˚C. Reactions were incubated at 27˚C for up to 120 minutes and placed on ice prior to visualization by HILO microscopy. Where indicated, the fusion inhibitors 3.2 µM Gyp1- 46 and 4 µM rGdi were added to block the reaction (see *Brett & Merz, 2008*). For heat stress treatment, isolated vacuoles were incubated at 37 ˚C for 5 minutes prior to adding them to reactions. Experimental data shown represent 3 or more biological replicates (each a smaple prepared from a separate yeast culture on different days) conducted in duplicate (technical replicates).

2.3.8 pHluorin-based internalization assay

Ecliptic pHluorin (a pH-sentivie variant of GFP) was tagged to the cytoplasmic C-terminus of Mup1 protein (*Prosser et al., 2010*). As previously described (*McNally et al., 2017*), 30 µL fusion reactions containing 6 µg isolated vacuoles and standard reaction buffer were prepared on ice and then transferred to pre-warmed black 96-well conical-bottom microtiter plates. pHluorin fluorescence was recorded every 2 minutes for up to 90 minutes at 27 ˚C using a BioTek Synergy H1 multimode plate reading fluorometer (BioTek Instruments, Whiting, USA). Data shown are representative traces with values normalized to initial readings at 0 minutes and represent 3 biological replicates (each a sample prepared from a spate yeast culture on different days) conducted in duplicate (technical replicates).

2.3.9 Data analysis and presentation

Movies and micrographs were processed using ImageJ and Adobe Photoshop CC software. Images presented were adjusted for brightness and contrast, inverted and sharpened with an unsharp masking filter. 3-dimensional or linear intensity profiles of GFP or FM4-64 fluorescence were generated using ImageJ software. Movie snapshots were selected to highlight docking and ILF formation during vacuole fusion. Group allocations were blinded for all micrographic analysis. Cellular pHluorin or GFP location measurements were conducted using the ImageJ Cell Counter plugin. Micrographic data was quantified by

counting total number of cells, as well as number of cells where the GFP fluorescence was detected on the plasma membrane, intracellular puncta, the vacuole membrane, or in the vacuole lumen. Values for each location were normalized to the total number of cells. Movies of vacuole fusion acquired in vivo were used to calculate the frequency of fusion events, reported as percentage of cells showing at least one event within 5 minutes; Only cells containing 2 or more vacuoles were counted.

Relative vacuole boundary, lumenal or outside membrane GFP fluorescence values were measured using ImageJ software as previously described (e.g. *McNally et al. 2017*). Prior to quantification, micrographs were background subtracted and a 4x4 pixel region of interest was then used to measure mean GFP fluorescence on the boundary membrane, in the lumen or on the outer membrane of docked vacuoles only. Single vacuoles or docked vacuoles without a clear outer membrane (i.e. those in large clusters) were excluded. Mean GFP fluorescence intensity over area (boundary length, lumenal area or vacuole circumference) was calculated by measuring vacuole diameter (average of two lengthwise measurements) and boundary membrane length. Mean boundary GFP fluorescence was normalized to mean outer membrane fluorescence, to assess enrichment or depletion, and lumenal GFP fluorescence was normalized to total fluorescence (sum of boundary, outer membrane and lumen). Only cells or reactions containing clearly resolved docked vacuole membranes were used for micrographic analysis. To assess membrane fusion in vitro, we calculated vacuole surface area using averaged diameter measurements before (t = 0 minutes) and after addition of ATP to trigger fusion. Organelles were assumed to be spherical, and products of homotypic fusion are predicted to be larger than donor organelles. When applicable, data are reported as column scatter plots as well as mean ± S.E.M. Comparisons were calculated using Student two-tailed *t*-tests; *P* values are indicated and $P < 0.05$ suggests significant differences. Samples sizes were tested to ensure adequate power using online software (http://www.biomath.info). Variance was assumed to be similar between groups compared. Data was plotted using R-studio 3.6.3 or Synergy KaleidaGraph 4.0 software and figures were prepared using Adobe Illustrator CC software.

2.4 RESULTS

2.4.1 Mup1 degradation triggered by methionine persists in an ESCRT mutant

Precise control of surface transporter protein activity by down–regulation is necessary to maintain cellular pools of free amino acids required for metabolism, proteostasis, and survival in response to changes in nutrient availability (*Jones et al., 2012; Babst, 2020*). In *S. cerevisiae* for example, the high-affinity methionine permease Mup1, a quintessential ESCRT-client protein, is down-regulated —cleared from the plasma membrane and degraded — by the MVB pathway in response to methionine in the

environment (*Lin et al., 2008; Keener & Babst, 2013; Guiney et al., 2016*). However, it is not clear if Mup1 degradation persists when ESCRT genes are deleted. To test this, we used western blot analysis to examine degradation of GFP-tagged Mup1, whereby proteolysis was detected by assessing free-GFP cleavage from Mup1 (see *Guiney et al., 2016*). As previously reported, Mup1-GFP is rapidly degraded after wild type cells are exposed to methionine (**Figure 2.1A**). Importantly, Mup1-GFP degradation after methionine addition was similar in cells lacking VPS36, a key subunit of ESCRT-II required for protein sorting into the MVB pathway (**Figure 2.1A** and B; *Babst et al., 2002*). To confirm that surface Mup1-GFP was delivered to the vacuole lumen for degradation, we first visualized live cells stained with FM4-64 (to label vacuole membranes) before and 30 minutes after methionine addition. In both wild type and *vps36*Δ cells, Mup1-GFP appeared in the lumen of vacuoles after treatment (**Figure 2.1C**). Thus, Mup1-GFP continues to be endocytosed and delivered to the vacuole lumen for degradation in absence of the ESCRT subunit VPS36.

2.4.2 Mup1 is deposited onto vacuole membranes when unrecognized by ESCRTs

If deleting VPS36 prevents sorting of Mup1-GFP into ILVs — a requisite of the MVB pathway — then how is it delivered to the vacuole lumen for degradation? One possibility is that it is rerouted to vacuole membranes, where it may be degraded by the ILF pathway which degrades other surface transporters **(Figure 2.1D**; *McNally & Brett, 2018*). To investigate, we monitored the cellular distribution of Mup1-GFP in live yeast cells over time after methionine addition (**Figure 2.1E**). In wild type cells, prior to treatment (0 minutes), Mup1-GFP is mostly found on the plasma membrane. 5 minutes after exposure, it accumulates on intracellular puncta representing endosomes. Then, after 30 minutes, Mup1-GFP is predominantly found within the lumen of vacuoles where it is catabolized by lumenal acid hydrolases. Consistent with Mup1-GFP being efficiently packaged into ILVs by ESCRTs, we find that it does not appear on vacuole membranes stained with FM4-64 (**Figure 2.1F**). However, when studying *vps36*Δ cells, we found that Mup1-GFP follows a similar trajectory (**Figure 2.1E**), albeit with two important exceptions: (1) Large Mup1-GFP and FM4-64 –positive puncta appeared adjacent to vacuole membranes, a hallmark phenotype of ESCRT deletion mutants (VPS class E; *Raymond et al., 1992*), confirming ILV formation was blocked at endosomes in these cells, and (2) Mup1-GFP aberrantly accumulates on vacuole membranes on route to the lumen (**Figure 2.1E** and **F**), which is not a trafficking intermediate of the MVB pathway.

To better visualize this intermediate, we replaced the cytoplasmic GFP tag on Mup1 with pHluorin, a pH-sensitive variant of GFP. When exposed to the acidic environment of the vacuole lumen, pHluorin fluorescence is quenched allowing better detection of Mup1-pHluorin on vacuole membranes (*Prosser et al., 2010*). As expected, we observe Mup1-

pHluorin clearly decorating vacuole membranes only in *vps36*Δ cells (**Figure 2.1G**). Upon closer examination of the population of cells imaged, we confirmed that nearly 50 % of *vps36*Δ cells studied presented Mup1-pHluorin on vacuole membranes after methionine addition, whereas no wild-type cells showed this phenotype (**Figure 2.1H**). Because the MVB pathway does not involve this trafficking intermediate, we propose that when ESCRTs fail to sort endocytosed Mup1-GFP into ILVs at endosomes, it remains on MVB/endosome perimeter membranes and, upon MVB- vacuole fusion, is deposited on vacuole membranes (see *Karim et al., 2018a*). Here it is likely sorted into the lumen for degradation by a secondary, fail-safe mechanism.

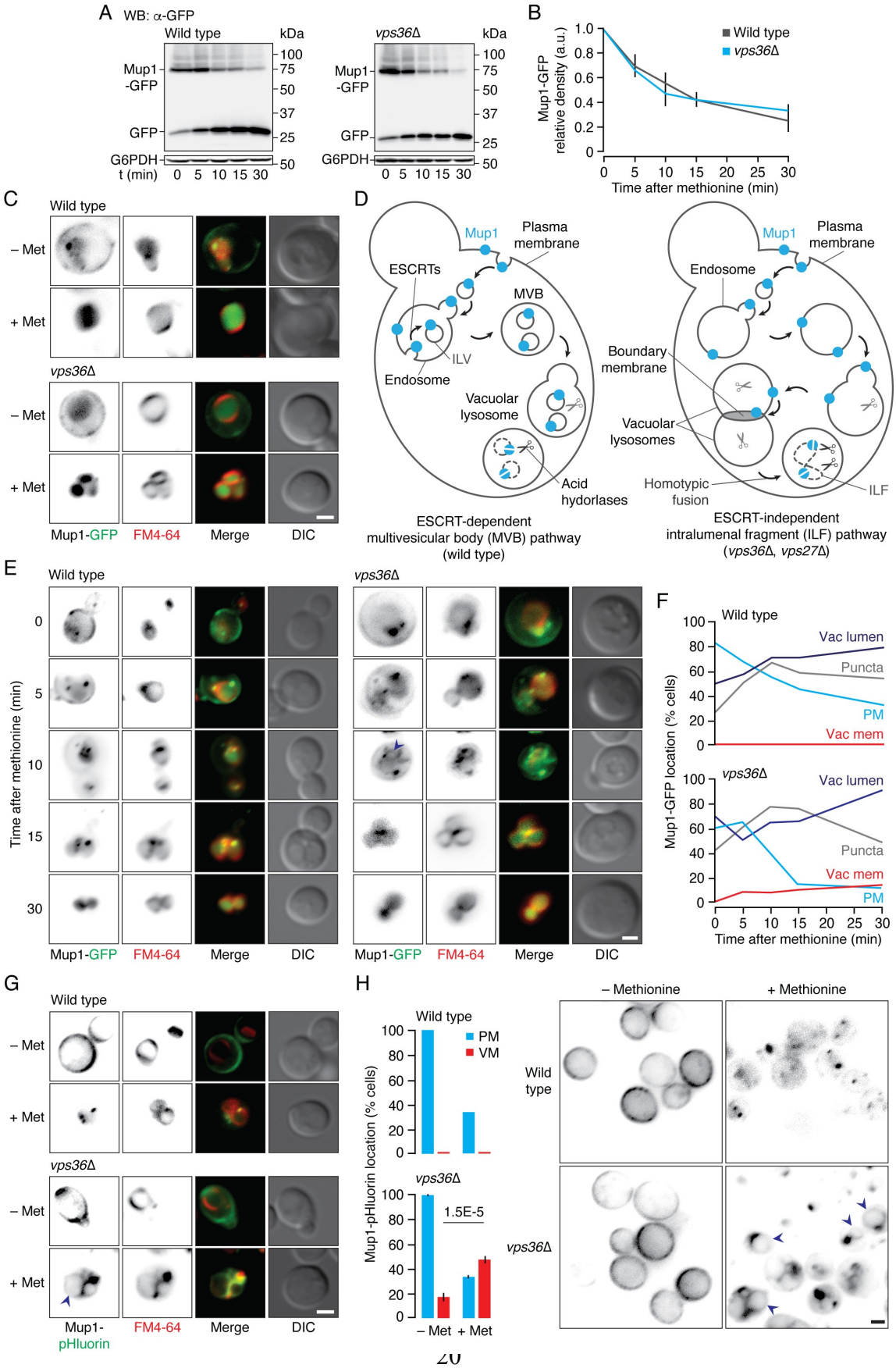
A
WB: α-GFP
Wild type
kDa
Mup1-GFP
GFP
G6PDH
t (min) 0 5 10 15 30
vps36Δ
100
75
50
37
25
B
Mup1-GFP relative density (a.u.)
Wild type
vps36Δ
Time after methionine (min)
C
Wild type
– Met
+ Met
vps36Δ
Mup1-GFP
FM4-64
Merge
DIC
D
Mup1
Plasma membrane
ESCRTs
MVB
ILV
Endosome
Vacuolar lysosome
Acid hydorlases
ESCRT-dependent multivesicular body (MVB) pathway (wild type)
Endosome
Boundary membrane
Vacuolar lysosomes
Homotypic fusion
ILF
ESCRT-independent intralumenal fragment (ILF) pathway (vps36Δ, vps27Δ)
E
Time after methionine (min)
0
5
10
15
30
F
Mup1-GFP location (% cells)
Vac lumen
Puncta
PM
Vac mem
G
Mup1-pHluorin
H
PM
VM
Mup1-pHluorin location (% cells)
1.5E-5
– Met
+ Met
– Methionine
+ Methionine
Wild type
vps36Δ

Figure 2.1. (previous page) Mup1 accumulates on vacuole membranes in *vps36*Δ cells after addition of methionine

(**A**)Western blot analysis of whole cell lysates prepared from wild type (WT) or *vps36*Δ cells expressing Mup1-GFP before (0 minutes) or 5 – 30 minutes after addition of methionine. Blots were stained for GFP or glucose-6-phosphate dehydrogenase (G6PDH; as load controls). Estimated molecular weights shown. (**B**) Intact Mup1-GFP band densities relative to 0 minutes and normalized to corresponding G6PDH densities were calculated for each time shown in A. n = 3 for each strain tested. (**C**) Fluorescence and DIC micrographs of live wild type or *vps36*Δ cells stained with FM4-64 and expressing Mup1-GFP before or 30 minutes after addition of methionine. (**D**) Cartoon illustrating how surface ESCRT-client proteins like Mup1 may be rerouted to the vacuole membrane and ILF pathway for degradation when MVB formation is blocked. (**E**) Fluorescence and DIC micrographs showing route taken by Mup1-GFP from the plasma membrane to the vacuole lumen in response to methionine over 30 minutes in live wild type or *vps36*Δ cells stained with FM4-64. (**F**) Proportion of wild type or *vps36*Δ cells that show Mup1-GFP fluorescence on the plasma membrane (PM), intracellular puncta, vacuole membrane (Vac mem) or vacuole lumen over time after methionine addition. n values for wild type (0, 5, 10, 20, 30 min) are 242, 327, 229, 267, 266 cells; *vps36*Δ are 216, 216, 214, 196, 222 cells. (**G**) Fluorescence and DIC micrographs of live wild type or *vps36*Δ cells stained with FM4-64 expressing Mup1-pHluorin before or 10 minutes after addition of methionine. (**H**) Proportion of wild type or *vps36*Δ cells that show Mup1-pHluorin fluorescence on the plasma membrane (PM) or vacuole membranes (VM) before or 10 minutes after methionine addition. Micrographs show Mup1-pHluorin location within cells. n values for wild type are 318, 304 cells; *vps36*Δ are 324, 348 cells analyzed before or after methionine addition respectively. Means ± S.E.M. and results from Student t-test are shown. Cells were stained with FM4-64 to label vacuole membranes. Arrowheads indicate Mup1-GFP or Mup1-pHluorin on vacuole membranes. Scale bars, 2 μm.

2.4.3 The ILF pathway mediates Mup1 down-regulation by methionine when ESCRTs are inactivated

Polytopic proteins that reside on vacuole membranes can be selectively degraded by three mechanisms: the VRED (vacuole membrane protein recycling and degradation) pathway, microautophagy, or the ILF pathway (*Li et al., 2015a; Zhu et al., 2017; McNally et al., 2017*). The presence of internalized Mup1-GFP on vacuole membranes suggests that at least one of these mechanisms is responsible for their degradation. However, the VRED and microautophagic pathways are ESCRT-dependent, eliminating the possibility that they contribute. Moreover, other surface transporters known to be down–regulated by the ESCRT–independent ILF pathway (e.g. Hxt3, a glucose transporter) appear on vacuole membranes after they are internalized by endocytosis (*McNally & Brett, 2018*). Thus, we hypothesized that the ESCRT– client Mup1-GFP is degraded by the ILF pathway in *vps36*Δ cells (see **Figure 2.2A**).

To be degraded by the ILF pathway, transporter proteins are sorted into an area of the vacuole membrane surrounded by a ring of fusogenic lipids and proteins assembled at the interface or "boundary" between apposing organelles (*Wang et al., 2013; Fratti et al., 2014; McNally et al., 2017*). We assessed Mup1-pHluorin sorting by measuring pHluorin fluorescence intensity within boundary membranes relative to its intensity in the membrane outside of this area using micrographs of *vps36*Δ cells treated with methionine. We found that Mup1-pHluorin was present within boundary membranes formed between docked vacuoles (**Figure 2.2B**) within the population of cells studied (**Figure 2.2C**). To better assess Mup1-pHluorin sorting into the ILF pathway, we compared it to GFP-tagged Fet5, a vacuolar copper-iron oxidase that is typically excluded from, or Fth1, a vacuolar iron transporter that is typically enriched in boundary membranes (see *McNally et al, 2017*). We found Mup1-pHlurorin levels were higher than Fet5- GFP but lower than Fth1-GFP (measured in either *vps36*Δ or wild types cells), suggesting that its sorting into boundary membranes is neither restricted or enhanced (**Figure 2.2B and C**), and like Fth1 and Fet5, Mup1 sorting into boundaries does not require ESCRTs (*McNally et al., 2017*). Nevertheless, the presence of Mup1-GFP in boundaries suggests it is degraded by the ILF pathway in cells lacking VPS36.

To internalize proteins into the lumen, docked vacuoles undergo homotypic lipid bilayer merger at the vertex ring that surrounds apposing boundary membranes to produce an ILF within the fusion product (*Wang et al., 2002; McNally et al., 2017*). To confirm that Mup1 is delivered to the vacuole lumen by this mechanism, we recorded homotypic vacuole fusion events in live *vps36*Δ cells exposed to methionine using HILO fluorescence

microscopy. As expected, Mup1-pHluorin decorating boundary membranes is internalized within an ILF upon homotypic vacuole fusion (**Figure 2.2D**). This is consistent with results from western blot analysis (**Figure 2.1A and B**) and delivery to the vacuole lumen (**Figure 2.1C**). Notably, methionine addition does not affect frequency of homotypic vacuole fusion events (**Figure 2.2E**), suggesting that stimulation of vacuole fusion itself is not required to accommodate Mup1 degradation. Thus, we conclude that methionine addition triggers Mup1 sorting into the ILF pathway for degradation when ESCRTs are inactive.

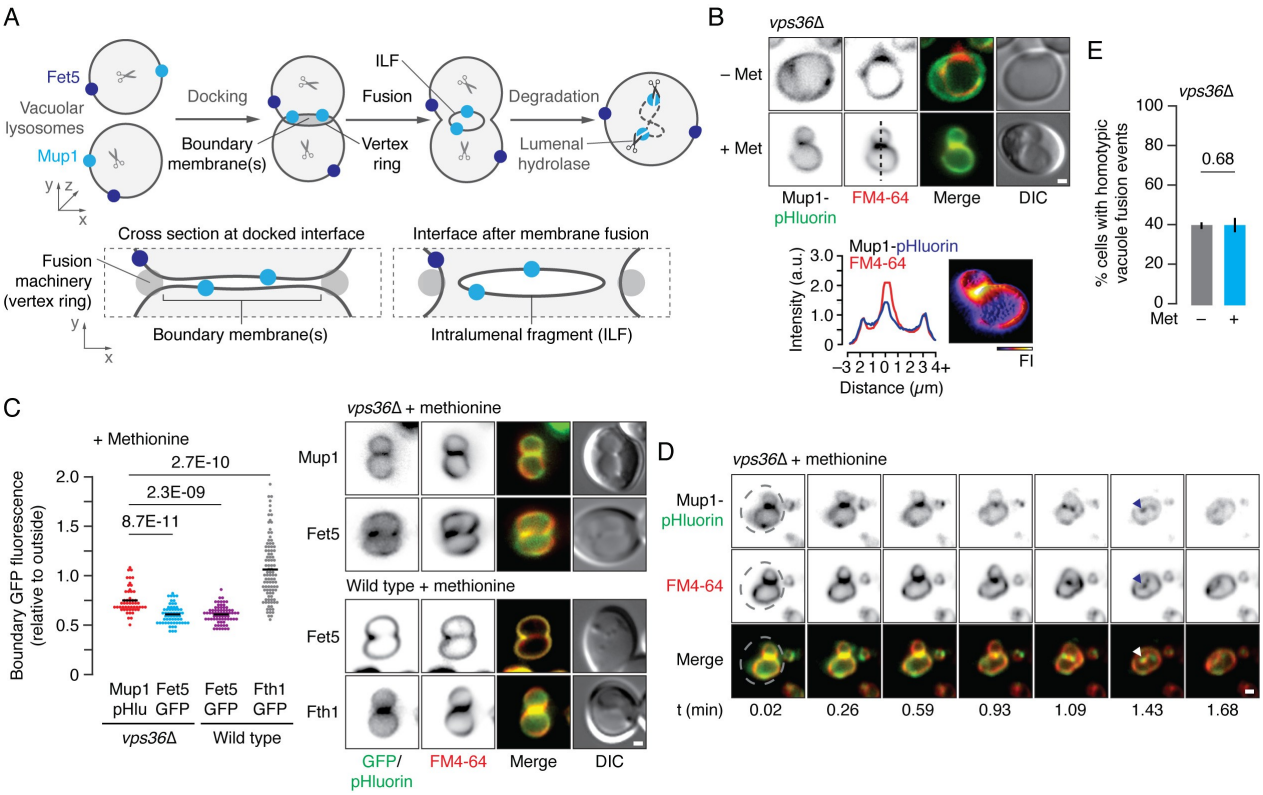

Figure 2.2. Methionine triggers Mup1 degradation by the ILF pathway in *vps36*Δ cells
(**A**) Cartoon illustrating how Mup1 on vacuole membranes may be sorted into boundaries and ILFs formed during homotypic vacuole fusion. Whereas Fet5 is depleted from boundaries and ILFs, and exclusively resides on outside membranes. (**B**) Fluorescence and DIC micrographs of live *vps36*Δ cells stained with FM4-64 expressing pHluorin-tagged Mup1 before or 10 minutes after addition of methionine. A 3-dimensional Mup1-pHluorin fluorescence intensity (FI) plot and line plots of pHluorin or FM4-64 (line shown in above micrograph) indicate boundary membrane localization after methionine addition. (**C**) Mup1-pHluorin, Fet5-GFP or Fth1-GFP fluorescence measured within boundary membranes of docked vacuoles within live wild type or *vps36*Δ cells in the presence of methionine. 52 (Mup1- pHluroin, *vps36*Δ), 82 (Fet5-GFP, *vps36*Δ), 70 (Fet5-GFP, wild type), 97 (Fth1-GFP, wild type) boundaries were analyzed. Mup1-pHluorin was absent from vacuole membranes without methionine and thus was not analyzed. (**D**) Snapshots from time-lapse movie showing a homotypic vacuole fusion event within a live *vps36*Δ cell expressing Mup1-pHluorin stained with FM4-64 10 minutes after methionine addition. Dotted lines indicate cell perimeter; arrowheads indicate newly formed ILF. (**E**) Analysis of data shown in **D** indicating proportion of *vps36*Δ cells that displayed a vacuole fusion event within 5 minutes before (n = 1,446) or 10 minutes after methionine addition (1,057). Means (bars) ±

S.E.M. and results from Student t-test are shown. Vacuole membranes were stained with FM4-64. Scale bars, 1 μm.

2.4.4 The ILF pathway degrades Mup1 in *vps36*Δ or vps27Δ cells for proteostasis

TOR (Target Of Rapamycin) signaling is a critical mediator of cellular proteostasis: when external amino acids are abundant TOR kinase is activated to replace high-affinity transporters (e.g. Mup1), critical for scavenging amino acids when cells are starved, with low-affinity transporters, to optimize nutrient uptake (*Babst & Odorizzi, 2013; Hatakeyama et al., 2019*). Thus, in response to adding methionine to methionine–starved cells, TOR signaling is activated to ubiquitylate Mup1 on the plasma membrane triggering endocytosis and degradation by the MVB pathway (*MacGurn et al., 2011*). External amino acid sensing can be bypassed by directly activating TOR signaling with cycloheximide to drive Mup1 ESCRT-mediated down–regulation (*Lin et al., 2008; Nikko & Pelham, 2009; MacGurn et al., 2011*). But it is unclear if TOR signaling continues to mediate Mup1 degradation by the ILF pathway in *vps36*Δ cells. Thus, we used HILO fluorescence microscopy to test if cycloheximide continued to induce Mup1 down–regulation in cells missing ESCRT genes. We first confirmed that cycloheximide triggers Mup1-pHluorin endocytosis in wild type cells (**Figure 2.3A**). When the MVB pathway is inactivated by deleting VPS36, Mup1-pHluorin endocytosis persists but it aberrantly accumulates on vacuole membranes (**Figure 2.3A and B**). Cycloheximide also stimulated delivery of Mup1-GFP to vacuole membranes in cells lacking VPS27, a component of ESCRT-0 (*Katzmann et al., 2003*), confirming that mutations targeting different ESCRT complexes show similar phenotypes (**Figure 2.3C**). Here, Mup1-GFP is present in boundaries formed between docked organelles (**Figure 2.3C and D**) that are internalized upon fusion (**Figure 2.3E**) and degraded (**Figure 2.3F and G**). Thus, activation of TOR signaling with cycloheximide triggers Mup1 clearance by the ILF pathway when ESCRTs are inactivated. This result is consistent with the idea that Mup1 ubiquitylation stimulated by TOR kinase is critical for endocytosis of surface Mup1, but is dispensable for directing Mup1 to ESCRTs after delivery to endosomes, as in their absence, Mup1 continues to be degraded by the ILF pathway.

Protein quality control is also critical for cellular proteostasis: Misfolded or damaged polytopic proteins that cannot be refolded by chaperones are cleared from the plasma membrane by the MVB pathway to prevent dysfunction and aggregation that may lead to cell death, and to replenish free amino acid pools for protein biosynthesis (*Babst, 2014*). Given that the ILF pathway is also responsible for degrading misfolded polytopic proteins (*McNally et al., 2017; McNally & Brett, 2018*), we hypothesized that it may mediate Mup1 protein quality control in cells lacking ESCRT activity. To trigger protein

misfolding, we subjected cells to acute, sublethal heat stress (42˚C for 30 minutes). After confirming Mup1-GFP degradation was stimulated by heat stress in wild type cells, we determined if the ILF pathway clears Mup1 in response to heat stress in *vps36*Δ or *vps27*Δ cells. As predicted, Mup1 is targeted to vacuole membranes and the ILF pathway for degradation after heat stress when ESCRTs are inactivated (**Figure 2.3A – G)**. Together, these results suggest that the ILF pathway compensates for loss of ESCRTs to ensure protein quality control and cellular proteostasis. Given that misfolded proteins continue to be cleared by the ILF pathway in the absence of ESCRTs, we hypothesized that this compensatory mechanism should prevent their toxic accumulation and aggregation, ultimately leading to cell death (*Babst, 2014*). If true, then deleting ESCRT genes should have no effect on cell survival after heat stress. To test this hypothesis, we measured cell viability by staining yeast cultures with methylene blue to detect dead cells before or after treatment with lethal heat stress (50 ˚C for 30 minutes). As expected, deleting VPS36 (ESCRT-II), VPS27 (ESCRT-0) or other ESCRT genes (VPS23, ESCRT-I; SNF7, ESCRT-III) had no effect on cell viability in response to heat stress as compared to wild type cells (**Figure 2.3H and I**). As positive controls, we found that heat stress killed most cells lacking genes encoding important protein chaperones activated by heat (SSA2 or HSC82, orthologs of Hsp70 and Hsp90 respectively; *Werner-Washburne et al., 1987; Borkovich et al., 1989*). As a negative control, deleting FET5, which encodes a copper-iron oxidase with no known role in the canonical heat shock response, has no effect on cell survival after lethal heat stress. All things considered, we conclude that the ILF pathway compensates for the loss of the MVB pathway by mediating surface amino acid transporter protein down-regulation for cellular proteostasis necessary for survival.

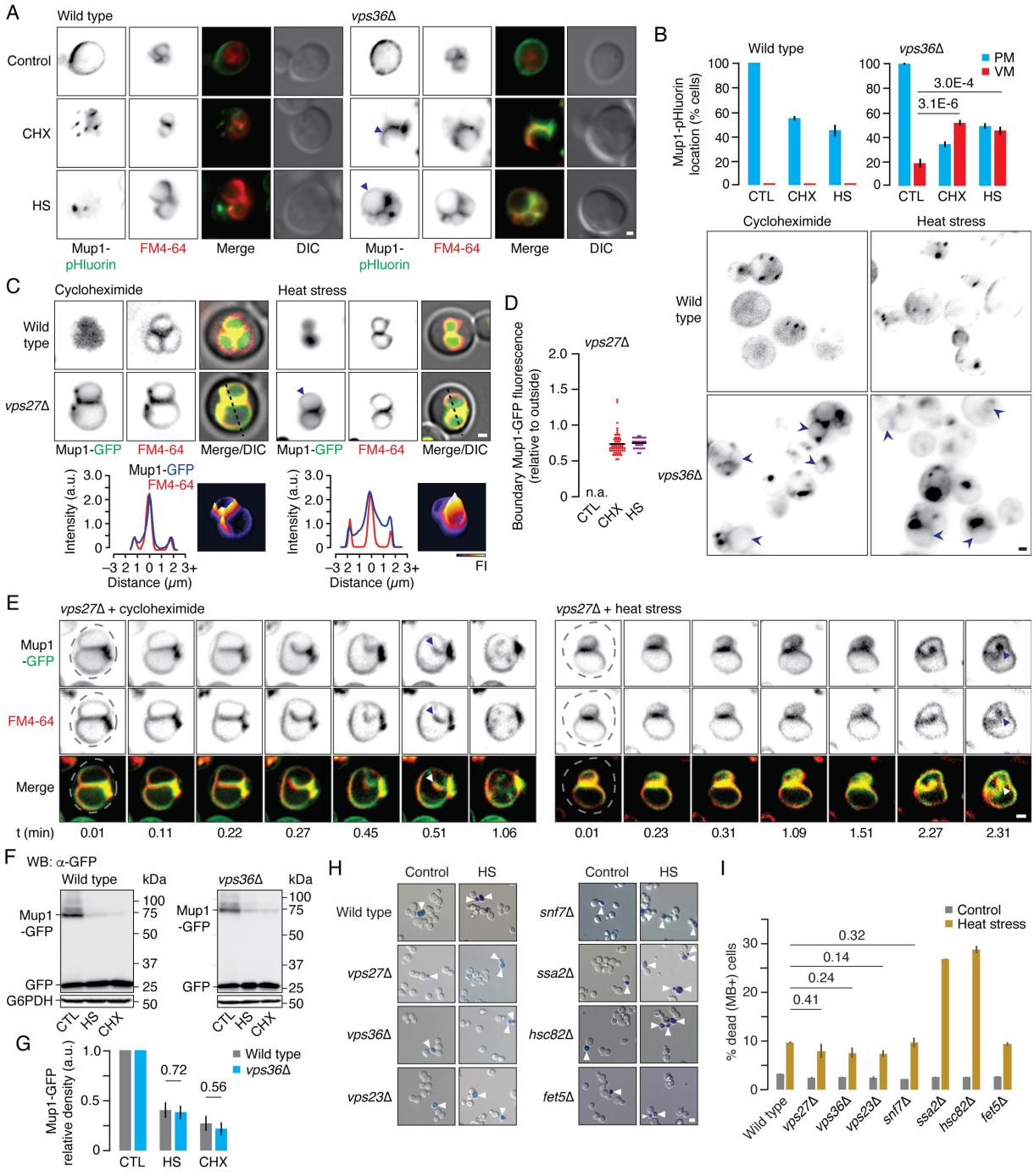

Figure 2.3. The ILF pathway degrades Mup1 in response to heat stress or cycloheximide in cells missing ESCRTs

(**A**)Fluorescence and DIC micrographs of live wild type or *vps36*Δ cells stained with FM4-64 expressing Mup1-pHluorin before (control) or after addition of 100 μM cycloheximide (CHX) or heat stress (HS; 42˚C for 15 minutes). Arrowheads indicate Mup1-pHluorin on

vacuole membranes. (**B**) Proportion of wild type or *vps36*Δ cells showing Mup1-pHluorin fluorescence on the plasma membrane (PM) or vacuole membranes (VM) before or after treatment with cycloheximide (CHX) or heat stress (HS). (below) Micrographs show Mup1-pHluorin location within cells; arrowheads indicate vacuole membranes. Number of cells analyzed (control, HS, CHX) are: WT (318, 315, 365), *vps36*Δ (324,327,339). (**C**) Fluorescence and DIC micrographs of live wild type or *vps27*Δ cells stained with FM4-64 expressing Mup1-GFP after addition of cycloheximide or heat stress. Three-dimensional Mup1-GFP fluorescence intensity (FI) plots and line plots of GFP or FM4-64 for lines shown above in micrographs indicate boundary membrane localization. (**D**) Mup1-GFP fluorescence measured within boundary membranes between docked vacuoles within live *vps27*Δ cells before (control; CTL) or after addition of cycloheximide (CHX) or heat stress (HS). Mup1-GFP was absent from vacuole membranes under control conditions and not analyzed (n.a.). Number of *vps27*Δ cells analyzed (HS, CHX) are: 60, 28. (**E**) Snapshots from time-lapse movies showing homotypic vacuole fusion events within live *vps27*Δ cells stained with FM4-64 expressing Mup1-GFP treated with cycloheximide or heat stress. Dotted lines indicate cell perimeters; arrowheads indicate newly formed ILFs. (**F**) Western blot analysis of whole cell lysates prepared from wild type or *vps36*Δ cells expressing Mup1-GFP before (control; CTL) or after heat stress (HS) or cycloheximide (CHX) treatment. Blots are stained with anti-GFP or anti-G6PDH antibodies. Estimated molecular weights are shown. (**G**) Intact Mup1-GFP band densities relative to control and normalized to load controls (G6PDH) were calculated for each condition shown in F. n = 3 for each strain tested. (**H**) Light micrographs showing methylene blue (MB) stained cultures of wild type, *vps27*Δ, *vps36*Δ, *vps23*Δ, *snf7*Δ, *ssa2*Δ, *hsc82*Δ, or *fet5*Δ cells before or after heat stress (HS). Arrowheads indicate MB-positive cells. (I) Images in H were used to measure proportion of dead, MB-positive cells in the population. Number of cells analyzed (control, HS) are: 3,232, 1,995 wild type; 2,023, 1,647 *vps27*Δ; 2,226, 1,548 *vps36*Δ; 1,877, 1,743 *vps23*Δ; 1,563, 1,470 *snf7*Δ; 3,305, 2,017 *ssa2*Δ; 3,401, 2,001 *hsc82*Δ; 2,061, 1,323 *fet5*Δ. Means (bars) ± S.E.M. and results from Student t-test are shown. Vacuole membranes were stained with FM4-64. Scale bars, 1 μm (except in H, 4 μm).

2.4.5 Mup1-GFP degradation requires ILF pathway machinery when ESCRTs are absent

Polytopic protein sorting into the ILF pathway relies on molecular machinery that co-purifies with vacuoles, in a preparation devoid of cytoplasmic factors that may contribute to Mup1 degradation (e.g. the proteasome) or biosynthesis (ribosomes, endoplasmic reticulum; *McNally et al., 2017; McNally & Brett, 2018*). Thus, to confirm that ESCRT-clients delivered to vacuole membranes uses the ILF machinery for degradation, we isolated vacuoles expressing Mup1– GFP from wild type cells or cells lacking VPS27 and stimulated homotypic vacuole fusion in vitro (by adding physiological salts and ATP; *Wickner, 2010*). We imaged reactions using HILO microscopy and first confirmed that no Mup1-GFP was observed on FM4-64-stained membranes of vacuoles isolated from wild type cells. Rather diffuse GFP fluorescence was exclusively detected in the lumen (as expected; **Figure 2.4A**) and this signal was constant over time suggesting no additional Mup1-GFP was internalized during the fusion reaction in vitro (**Figure 2.4B**). However, in vacuoles freshly isolated from *vps27*Δ cells, we found that relatively less Mup1-GFP was in the lumen, which correlated with its presence on outside membranes (**Figure 2.4A**). Importantly, outside membrane GFP decreased, whereas lumenal GFP and vacuole size increased over time (**Figure 2.4B and C**) consistent with Mup1-GFP internalization upon homotypic fusion of vacuoles isolated from *vps27*Δ cells triggered by ATP in vitro. Also, FM4- 64-postive vesicles accumulated in the lumen of vacuoles over time, likely representing ILFs formed during homotypic vacuole fusion in vitro (**Figure 2.4A**). Notably, Mup1-GFP only appears on ILFs within vacuoles isolated from *vps27*Δ cells over time. These results confirm that selective delivery of Mup1-GFP from the vacuole membrane into its lumen is ESCRT- independent and the underlying machinery co–purifies with the organelles. Heat stress triggers endocytosis of surface transporter proteins required for delivery to vacuoles for degradation (**Figure 2.3**). However, it is unclear whether signaling mechanism triggered by these stimuli also directly facilitate client protein recognition on intracellular membranes by ESCRTs. Whereas, we previously showed that the ILF machinery on isolated vacuole membranes can directly respond to multiple stressors to promote protein degradation (*McNally et al., 2017; Karim et al., 2018b; McNally & Brett, 2018*). This is consistent with the vacuole membrane being a major site for TOR signaling protein complex recruitment and assembly for activation (*Hatakeyama et al., 2019*), and key ubiquitylation machinery and molecular chaperones are known to reside on vacuole membranes (*Li et al., 2015b; Yang et al., 2020*). Thus, we hypothesized that the sorting and degradation machinery responsible for Mup1-GFP degradation may be directly stimulated by protein misfolding (heat stress). To test this hypothesis, we isolated vacuoles from unstimulated cells, treated them with heat stress under fusogenic conditions, and determined if Mup1-GFP degradation by the ILF pathway was enhanced in vitro.

In support, we found that more Mup1-GFP was enriched in boundary membranes between docked vacuoles isolated from *vps27*Δ cells after heat stress applied in vitro (**Figure 2.4D and E**), suggesting that protein sorting is stimulated at the vacuole membrane. Next, to determine if internalization was enhanced, we monitored Mup1-pHluorin fluorescence over the course of the fusion reaction (*McNally et al., 2017*). Internalization was observed as a decrease in fluorescence that occurs when pHluorin transitions from the relative high pH within the reaction buffer (pH 6.80) to low pH within the vacuole lumen (pH ~ 5.0). As expected, Mup1- pHluorin fluorescence decreases over time when vacuoles isolated from *vps27*Δ cells undergo fusion in vitro, and treatment with heat stress enhances this effect, particularly the initial rate of internalization (**Figure 2.4F**). Notably, pHluorin fluorescence does not change during fusion of vacuoles isolated from wild type cells, confirming our observation that Mup1-pHluorin is exclusively located in the lumen. Consistent with these results, heat stress stimulated Mup1- GFP accumulation in the lumen of vacuoles isolated from *vps27*Δ cells after fusion in vitro (**Figure 2.4G**). Moreover, western blot analysis showed cleavage of GFP from Mup1-GFP observed after 90 minutes of vacuole fusion in vitro was enhanced after heat stress (**Figure 2.4H**). Together, these results suggest that protein quality control mechanisms known to drive endocytosis of presumably misfolded surface Mup1-GFP may also activate machinery on vacuole membranes to optimize its degradation when ESCRTs are dysfunctional.

Activation of the resident vacuolar Rab-GTPase Ypt7 is implicated in sorting proteins into the ILF pathway prior to membrane fusion (*McNally et al., 2017*). Thus, if Mup1-GFP is down–regulated by the ILF machinery then inhibition of Ypt7 should block its degradation. To test this hypothesis, we acutely blocked Ypt7 by adding two purified recombinant protein inhibitors to vacuoles isolated from *vps27*Δ cells: rGdi1, which extracts Ypt7 from membranes rendering it inactive, and rGyp1-46, the catalytic domain of the Rab-GTPase activating protein Gyp1 that inactivates Ypt7 (*Brett & Merz, 2008*). As expected, we found that these Ypt7 inhibitors blocked Mup1-GFP sorting into boundary membranes (**Figure 2.4D and E**), Mup1- pHuorin internalization (**Figure 2.4F**), Mup1-GFP lumenal accumulation (**Figure 2.4G**) and its proteolysis (**Figure 2.4H**) under standard conditions or after further stimulation by heat stress. These results confirm that Mup1 degradation requires the ILF machinery when ESCRTs are defective.

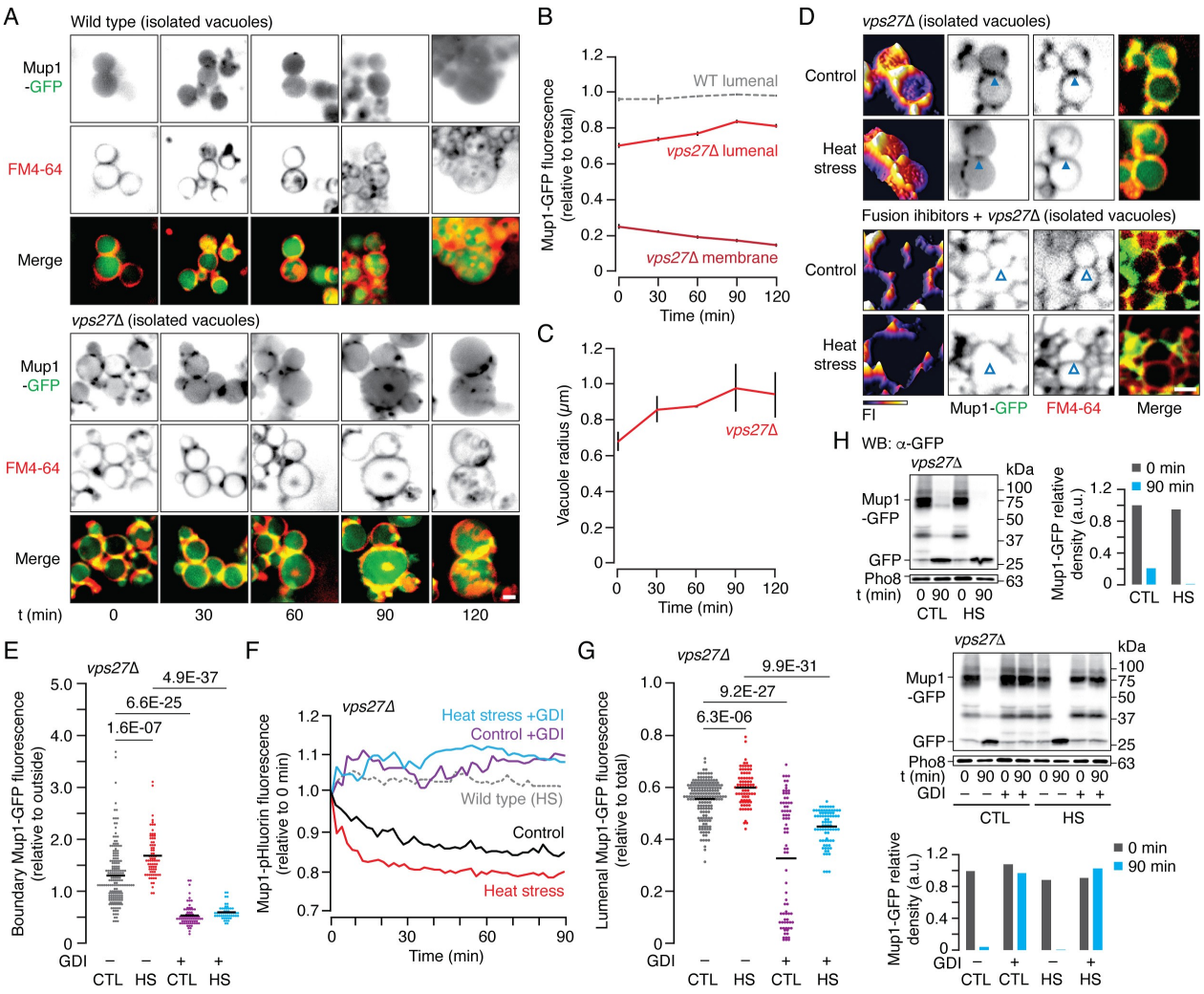

Figure 2.4. Molecular machinery for Mup1 degradation by the ILF pathway co-purifies with vacuoles

(**A**)Fluorescence micrographs of vacuoles isolated from wild type or *vps27*Δ cells expressing Mup1-GFP before (0 minutes) or after up to 120 minutes of fusion. Vacuole membranes were stained with FM4-64. (**B,C**) Vacuole radius (**C**) or Mup1-GFP fluorescence measured within the lumen or on outside membranes of vacuoles (**B**) isolated from wild type (WT) or *vps27*Δ cells before (0) or after fusion (up to 120 minutes). n values for 0, 30, 60, 90,120 minutes are 63, 52, 83, 115, 114 (WT); 93, 177, 128, 126, 104 (*vps27*Δ) vacuoles analyzed. (**D**) Fluorescence micrographs of vacuoles isolated from *vps27*Δ cells expressing Mup1-GFP after 30 minutes of fusion in the absence (control) or presence of heat stress (HS), and with or without fusion inhibitors (4 μM rGdi1 and 3.2 μM rGyp1-46). Vacuole membranes were stained with FM4- 64 and 3-dimensional fluorescence intensity (FI) plots of Mup1-GFP are shown. Arrowheads indicate boundary membranes

either enriched with (closed) or depleted of (open) Mup1-GFP. (**E, G**) Mup1-GFP fluorescence measured within boundary membranes (**E**) or the lumen (**G**) of vacuoles isolated from *vps27*Δ cells in the absence (control; CTL) or presence of heat stress (HS), and with or without fusion inhibitors (GDI) after 30 minutes of fusion. n values for CTL, HS are 176, 76 vacuoles analyzed without GDI; 73, 52 with GDI. (**F**) Relative fluorescence of vacuoles isolated from WT or *vps27*Δ cells expressing Mup1-pHluorin recorded over time during homotypic vacuole fusion in vitro in the absence (control; CTL) or presence of heat stress (HS) and with or without fusion inhibitors (GDI). n = 3 for each condition, representative traces shown. (**H**) Western blot analysis of Mup1-GFP degradation before (0) or after (90 minutes) fusion of vacuoles isolated from *vps27*Δ cells in the absence or presence of heat stress (HS) pretreated without (top) or with (bottom) fusion inhibitors (GDI). Blots were stained with antibodies to GFP or Pho8 (load control). Estimated molecular weights indicated. Intact Mup1-GFP band densities relative to control (0 min) normalized to load controls were calculated for each condition shown. n = 3 for each condition tested. Means (bars) ± S.E.M. and results of Student t-tests are shown. Scale bars, 1 μm.

2.4.6 Degradation of the G-protein coupled receptor Ste3 is mediated by MVB and ILF pathways

To demonstrate that surface receptor proteins, in addition to transporters, rely on the ILF pathway for down–regulation when the MVB pathway is impaired, we examined cells expressing GFP-tagged Ste3, a surface G-protein coupled receptor, and classical ESCRT-client, that is constitutively degraded by the MVB pathway (*Davis et al., 1993; Shields et al., 2009*). In untreated wild type cells, Ste3-GFP is present on the plasma membrane and within the vacuole lumen, which correlates with a relatively large proportion of cleaved GFP (versus full length Ste3-GFP) observed by western blot analysis (**Figure 2.5A**). As predicted, degradation of Ste3- GFP persists in unstimulated *vps27*Δ cells (**Figure 2.5A**), where it accumulates on vacuole membranes (**Figure 2.5B and C**). We made similar observations when treating cells with heat stress to further stimulate Ste3-GFP degradation (**Figure 2.5A – C**). Like Mup1 in *vps27*Δ cells, Ste3-GFP was present in boundary membranes between docked vacuoles (**Figure 2.5C and D**) where it was internalized into the lumen upon homotypic vacuole fusion (**Figure 2.5E and F**). Thus, we conclude that the ILF pathway is capable of mediating down–regulation of the receptor protein Ste3 when unrecognized by ESCRTs.

When we repeated these experiments with pHluorin in place of GFP to better assess the presence of Ste3 on vacuole membranes (without interference of fluorescence signal from the lumen), we discovered that Ste3-pHluorin sometimes appeared on vacuole membranes in wild type cells, whether unstimulated (6 % cells examined) or treated with heat stress (16 % cells; **Figure 2.5G – I**). This important finding proposes that even in the presence of ESCRTs, the ILF pathway may in part contribute to Ste3 down–regulation in wild-type cells (see **Figure 2.6**).

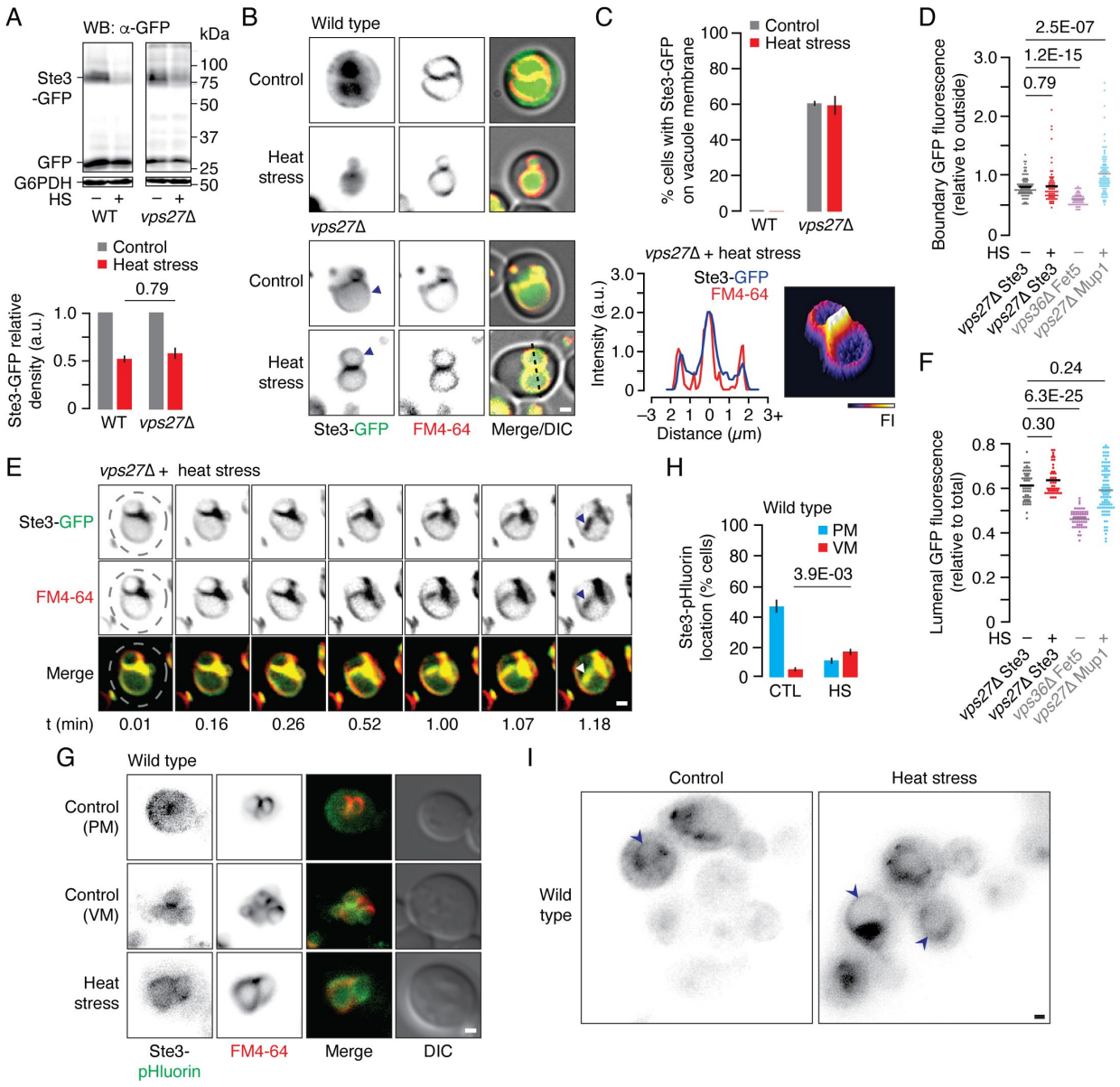

Figure 2.5. MVB and ILF pathways mediate degradation of Ste3

(**A**)Western blot analysis of whole cell lysates prepared from wild type (WT) or *vps27*Δ cells expressing Ste3-GFP that were untreated or exposed to heat stress (HS). Blots were stained for GFP or G6PDH (load controls). Estimated molecular weights are shown. Intact Ste3-GFP band densities relative to control and normalized to corresponding G6PDH densities were calculated. n = 3 for each strain tested. (**B**) Fluorescence and DIC micrographs of live wild type or *vps27*Δ cells stained with FM4-64 expressing Ste3-GFP before (control) or after heat stress (HS). Arrowheads indicate vacuole membranes. (**C**) Proportion of WT or *vps27*Δ cells that show Ste3-GFP fluorescence on vacuole membranes

before (control) or after heat stress. 885, 964 WT and 284, 166 *vps27*Δ cells were analyzed before or after heat stress respectively. A 3-dimensional Mup1-GFP fluorescence intensity (FI) plot and line plots of GFP or FM4-64 for line shown in B indicate vacuole and boundary membrane localization. (**D,F**) Ste3-GFP fluorescence measured within boundary membranes (**D**) or lumen (**F**) of vacuoles within live *vps27*Δ cells before (n = 93) or after heat stress (HS; n = 73). For comparison, boundary fluorescence of Fet5-GFP in *vps36*Δ or Mup1-GFP in *vps27*Δ cells after methionine addition are shown (**see Figure 2.2C**). (**E**) Snapshots from a time-lapse movie showing a homotypic vacuole fusion event within a live *vps27*Δ cell stained with FM4-64 expressing Ste3-GFP after heat stress. Dotted line indicates cell perimeter; arrowhead indicates newly formed ILF. (**G**) Fluorescence and DIC micrographs of live wild type cells stained with FM4-64 expressing Ste3-pHluorin before (control) or after heat stress. (**H**) Proportion of wild type cells that show Ste3-pHluorin fluorescence on the plasma membrane (PM) or vacuole membranes (VM) before (control, CTL; n = 195) or after heat stress (HS; n = 198). (**I**) Micrographs show Ste3-pHluorin location within cells; arrowheads indicate vacuole membranes. Means (bars) ± S.E.M. and results of Student t-tests are shown. Cells were stained with FM4-64 to label vacuole membranes. Scale bars, 1 μm.

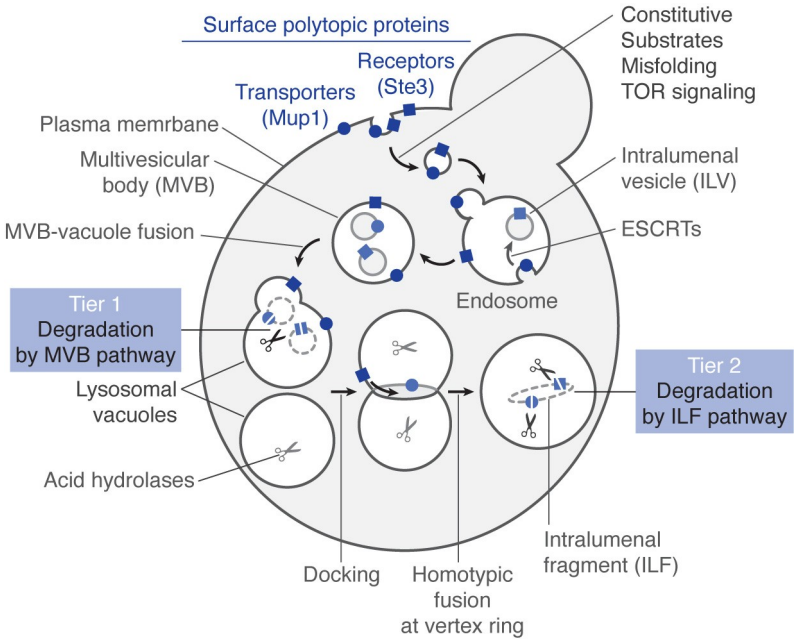

Figure 2.6. A two-tiered system ensures surface polytopic protein down-regulation
Cartoon illustrating how surface transporter and receptor proteins like Mup1 and Ste3, respectively, are degraded by a two-tiered system consisting of the MVB and ILF pathways.

2.5 Discussion

2.5.1 A new two-tier model for surface receptor and transporter down-regulation

Prior to this study, we discovered that the ILF pathway selectively down–regulates half of surface polytopic proteins studied (3 of 6) in wild type *S. cerevisiae* cells, including transporters for sugars (Hxt3), myo-inositol (Itr1) and amino acids (Aqr1; *McNally & Brett, 2018*). The remainder included Mup1 and Ste3, quintessential ESCRT-clients known to be degraded by the MVB pathway. Deleting ESCRT genes to block the MVB pathway, had no effect on ILF-client protein degradation, confirming that the underlying sorting machinery must be distinct. Thus, these two processes seemed to function independently, whereby each pathway was responsible for downregulating a unique subset of surface client proteins. If this existing model is accurate, then ESCRT-client protein down-regulation should be blocked when the MVB pathway is disrupted by genetic mutation.

Herein, we tested this hypothesis and provide extensive evidence that it is false: After down-regulation was triggered by multiple stimuli, both ESCRT-client proteins studied (Mup1, Ste3) continued to be delivered to the vacuole lumen and degraded in mutant cells. After endocytosis, they were aberrantly deposited on vacuole membranes, as observed, but not discussed in previous reports (e.g. *20 Bryant et al., 1998; Chen & Davis, 2002; Shaw et al., 2003; Yeo et al., 2003; Shields et al., 2009; Teis et al., 2010; Wrasman et al., 2018*), likely due to MVB/endosome–vacuole membrane fusion which is less efficient when ESCRTs are deleted (*Karim et al., 2018a*), but not completely blocked as previously implicated (e.g. *Piper et al., 1995*). This location does not represent a trafficking intermediate in the MVB pathway, implying that a secondary, ESCRT-independent process is responsible their down-regulation. Using many approaches, we demonstrate that these proteins are degraded by the ILF pathway. In particular, we visualized pHluorin– or GFP– tagged proteins being internalized on newly formed intralumenal fragments during homotypic vacuole membrane fusion events in live mutant cells. This unambiguously shows that ESCRT-client proteins are sorted for degradation by the ILF pathway when they are not sorted into the MVB pathway. Importantly, the G-protein coupled receptor Ste3 seems to be degraded by the ILF pathway in some wild type cells (**Figure 2.5**), suggesting that this secondary pathway may contribute to ESCRT-client protein degradation even when the MVB pathway is intact.

With these new observations in mind, we propose that a two-tier system mediates

surface receptor and transporter down–regulation (**Figure 2.6**): After endocytosis, proteins first encounter ESCRTs on endosome membranes and can be sorted into ILVs and the MVB pathway. If not detected, they remain on the MVB perimeter membrane and upon heterotypic fusion are deposited on vacuole/lysosome membranes. Here they are cleared by the ILF pathway. This fail–safe mechanism ensures all proteins are degraded.

We speculate that the ILF pathway represents a default mechanism for surface protein down–regulation, because lysosome physiology is reliant on membrane fusion: Lysosomes and vacuoles must undergo heterotypic membrane fusion to receive biomaterials from endocytic and autophagy pathways (*Nickerson et al., 2009; Karim et al., 2018a*). They undergo homotypic fusion (and fragmentation) to regulate their morphology – size, shape and number – necessary for organelle inheritance or compartmental expansion for example (*Li & Kane, 2009*). The machinery underlying these different fusion events is thought to be nearly identical (*Wickner, 2010; Balderhaar & Ungermann, 2013; Gao et al., 2018; Karim et al., 2018a*), suggesting that ILFs may be generated during heterotypic as well as homotypic fusion. ILF formation during homotypic lysosome fusion can be regulated: Some fusion events do not produce visible ILFs in unstimulated cells (*Wang et al., 2002; Mattie et al., 2017; Karim et al., 2018b*). Whereas, in addition to promoting protein sorting into ILFs, stressors increase the probability of ILF formation without changing frequency of fusion events (*Karim et al., 2018b*). This also seems to be the case for Mup1 degradation after methionine addition, as this stimulus did not affect frequency of vacuole fusion events (**Figure 2.2E**). Thus, every lysosomal fusion event required for organelle function or homeostasis, offers an opportunity to discard unneeded or damaged proteins by sorting them into ILFs. This includes newly deposited surface proteins which are likely recognized as foreign (non-resident, mislocalized) and cleared from lysosome membranes by the ILF pathway to maintain organelle identity.

On the other hand, since their discovery, ESCRTs have been observed at many sites within cells where they contribute to diverse processes besides the MVB pathway, from cytokinesis to plasma membrane repair to extraction of nuclear pore complexes (*Henne et al., 2011; Hurley, 2015; Vietri et al., 2019*). Not all ESCRT-client proteins decorating ILVs will necessarily be catabolized, as some MVBs fuse with the plasma membrane, releasing ILVs as extracellular vesicles to mediate intercellular signaling (*Votteler & Sundquist,* 2013; Juan *& Fürthauer, 2018*). Thus, we speculate that ESCRTs perhaps play a secondary, specialized role in surface protein down–regulation. For example, by acting relatively early in the endocytic pathway, ESCRTs may be limited to recognizing internalized surface client proteins that require immediate sequestration upon endocytosis to quickly terminate signaling (e.g. GPCRs), or to clear proteins that may disrupt function or integrity of endocytic organelles (*Dores & Trejo, 2019*). Although further study is required to better

elucidate their distinct roles in proteostasis it is now clear that both the MVB and ILF pathways are important contributors to surface polytopic protein down–regulation

2.5.2 How are client proteins recognized by both pathways?

To be recognized and sorted into the MVB pathway, ESCRT-client proteins are labeled with ubiquitin (*MacDonald et al., 2012*; *Lin et al., 2008; Nikko and Pelham, 2009*). On the other hand, mechanisms responsible for protein labeling and sorting into ILFs have not been elucidated. However, these new results offer insight into this process: Herein, we show that the ILF pathway degrades surface proteins known to be labeled with ubiquitin, consistent with previous results (*McNally & Brett, 2018*). Also, the ILF pathway responds to the same stimuli that trigger protein ubiquitylation for entry into the MVB pathway (*Nikko and Pelham, 2009; Keener and Babst, 2013; MacGurn et al., 2011; Jones et al., 2012; McNally et al., 2017; McNally & Brett, 2018*). For example, in response to amino acids, TOR signaling is activated to dephosphorylate the alpha-arrestin Art1, an adapter protein, which then binds Mup1 to promote ubiquitylation by the HECT E3 ubiquitin ligase Rsp5, a Nedd4 ortholog (*Ghaddar et al., 2014; Guiney et al., 2016; Gournas et al., 2017; Lee et al., 2019*). Notably client protein ubiquitylation is required for endocytosis (although contentious; e.g. *Chen & Davis, 2002*), and this process does not require ESCRTs (*Hicke & Riezman, 1996*; *MacGurn et al., 2012*). In support, we find that client protein endocytosis and upstream signaling mechanisms remain intact in cells missing ESCRTs when they are degraded by the ILF pathway (see **Figures 2.1, 2.2, 2.3 and 2.5**). From this perspective, both pathways seem to rely on protein ubiquitylation at the surface to drive endocytosis, a requisite for delivery to vacuolar lysosomes.

At endosomes, ubiquitylated surface receptor or transporter proteins are added to a complex membrane protein landscape that includes resident polytopic proteins, biosynthetic proteins on route to lysosomes, and proteins marked for degradation from other cell compartments. Here, at this major traffic intersection, functional proteins can be deubiquitylated and returned to the plasma membrane or their site of origin (i.e. recycled), or remain ubiquitylated to be sorted into ILVs by ESCRTs for degradation. However, this original binary model has since become contentious, as recent data questions the requirement of original ubiquitin labels for protein sorting into ILVs (e.g. *Babst, 2014*) or suggests a secondary intracellular labeling event may be required for ESCRT recognition after endocytosis (see *MacGurn et al., 2012; MacDonald et al., 2012; Dores & Trejo, 2018*).

Our findings also challenge this model by bringing attention to a third option, whereby some internalized surface proteins can be ignored by ESCRTs and retrograde trafficking mechanisms, remain on perimeter membranes of maturing MVBs, and after MVB-vacuole fusion, appear on vacuole membranes. Here, the molecular machinery can directly respond to stimuli to promote client protein degradation by the ILF pathway (**Figure 2.4**; also see *McNally et al., 2017; McNally & Brett, 2018*). Like endosomal membranes, protein labeling machinery is also found on vacuole membranes (*Li et al., 2015a; Li et al., 2015b*; *Sardana et al., 2019; Yang et al., 2020*). This supports the idea that labeling machinery present on endosome or vacuolar lysosome membranes likely contributes to sorting of client proteins into the MVB or ILF pathways for degradation.

What stimulates protein sorting into ILFs on vacuole membranes? One possibility is a proposed mechanism to protect organelle membrane identity: Extracellular faces of receptor or transporter proteins are glycosylated with different sugars and linkages than those covalently attached to lumenal faces of resident vacuole transporter proteins (*Stanley et al., 2017*). The surface-specific sugar groups may not offer protection from attack by lumenal hydrolases. Thus, we speculate that, upon delivery to vacuole membranes, surface proteins are particularly susceptible to cleavage, triggering misfolding, which in turn recruit mechanisms on the vacuole membrane to label and sort them into the ILF pathway. Although speculative, this model is supported by the observation that heat stress, to promote misfolding, applied to vacuole fusion reactions further stimulates Mup1 degradation in vitro (**Figure 2.4**). How misfolded proteins are then recognized is unclear, but is the focus of ongoing studies important for understanding how ILF and MVB pathways share the burden of surface transporter and receptor down-regulation.

2.5.3 Relevance to physiology and disease

Selective down-regulation of surface receptor, transporter and channel proteins triggered by second messenger signaling or substrates underlies diverse physiology in all eukaryotes. Thousands of genes, more than 30% of eukaryotic genomes, are thought to encode membrane proteins (e.g. *Fagerberg et al., 2010*). However, the degradation of only a few surface membrane proteins has been studied in molecular detail. In particular, evidence directly implicating ESCRTs and the canonical MVB pathway in this process is scarce. Herein we show that two of the best characterized ESCRT-clients can be degraded by the ILF pathway, either constitutively or to accommodate proteostasis and protein quality control, fundamental processes necessary for cell survival (**Figures 2.1 – 2.5**). Misfolded proteins that supposedly evade endoplasmic-reticulum-associated degradation (ERAD) can

also be delivered to the MVB pathway for clearance (e.g. Slg1; *Wang et al., 2011*). When this is blocked, they accumulate on vacuole membranes and may be degraded by the ILF pathway, possibly broadening its role in cellular protein quality control. Properly delivery of biosynthetic cargo proteins (e.g. acid hydrolases, polyphosphatases) to the vacuole lumen also relies on the MVB pathway (*Odorizzi et al., 1998; Katzmann et al., 2001*). ESCRT mutations result in their aberrant deposition on vacuole membranes as well (e.g. Cps1 or Ppn1; *Odorizzi et al., 1998; Reggiori & Pelham, 2001; Babst et al., 2002; Katzmann et al., 2004; McNatt et al., 2007; Shields et al., 2009; Ren & Hurley, 2010; Yang & Hurley, 2010; Ren & Hurley, 2011; Mageswaran et al., 2015*). This suggests that the ILF pathway may also act as a secondary mechanism for biosynthetic cargo delivery; a focus of ongoing studies aimed at better understanding its broader roles in organelle homeostasis. But as it stands, it seems that the ILF pathway may play an equally important role in physiology as the canonical MVB pathway, as key components of a two-tiered system for selective lysosomal degradation of polytopic proteins.

Lumenal vesicles that resemble ILFs within lysosomes have been observed in organisms ranging from yeast to plants to humans, since the discovery of this organelle decades ago (also called "dense bodies", e.g. *Novikoff et al., 1956*). It is not currently resolved if they are products of membrane fusion or ESCRTs. However, all known machinery underlying ILF formation is conserved in all eukaryotes (*Balderhaar & Ungermann, 2013; Karim et al., 2018b*).

Similar to our findings in *S. cerevisiae*, surface receptor proteins accumulate on vacuole membranes when ESCRT genes (e.g. CHMP1) are deleted in plants including PIN1, PIN2 and AUX1 which are critical for auxin signaling underlying development (*Otegui, 2018*). Thus, it is possible that a similar two-tiered system is at play in plant cells. Loss-of-function mutations in human ESCRT genes are linked to cancers and neurodegenerative disorders, and it was proposed that etiology may involve improper client protein down–regulation (*Saksena and Emr, 2009; Stuffers et al., 2009a; Alfred and Viccari, 2016*). For example, pathogenesis of cancers could be driven by improper surface integrin protein degradation, preventing termination of oncogenic signaling, as implicated in sporadic lung adenoma (*Manteghi et al., 2016*). Whereas, ESCRT mutations could promote gradual accumulation and possible aggregation of surface proteins causing neural cell dysfunction and premature cell death, a common mechanism thought to underlie neurodegenerative diseases (*Kaul & Chakrabarti, 2017*). Although defects in other ESCRT-mediated cellular processes may contribute to pathology (*Raiborg & Stenmark, 2009*), our findings offer a new potential therapeutic strategy to possibly overcome defects in protein down–regulation by targeting the ILF pathway, e.g. through TFEB (Transcription Factor EB) to increase lysosome numbers and/or fusogenicity (*Ferguson, 2015; Napolitano and Ballabio, 2016*).

References

Abu-Remaileh, M., Wyant, G. A., Kim, C., Laqtom, N. N., Abbasi, M., Chan, S. H., Freinkman, E., & Sabatini, D. M. (2017). Lysosomal metabolomics reveals V-ATPase- and mTOR-dependent regulation of amino acid efflux from lysosomes. *Science (New York, N.Y.)*, *358*(6364), 807–813.

Adell, M. A., Vogel, G. F., Pakdel, M., Müller, M., Lindner, H., Hess, M. W., & Teis, D. (2014). Coordinated binding of Vps4 to ESCRT-III drives membrane neck constriction during MVB vesicle formation. *The Journal of cell biology*, *205*(1), 33–49.

Aerts, J., Kuo, C. L., Lelieveld, L. T., Boer, D., van der Lienden, M., Overkleeft, H. S., & Artola, M. (2019). Glycosphingolipids and lysosomal storage disorders as illustrated by gaucher disease. *Current opinion in chemical biology*, *53*, 204–215.

Alfred, V., and Vaccari, T. (2016). When membranes need an ESCRT: endosomal sorting and membrane remodelling in health and disease. *Swiss Med. Wkly. 146*, w14347.

Amerik, A. Y., Nowak, J., Swaminathan, S., & Hochstrasser, M. (2000). The Doa4 deubiquitinating enzyme is functionally linked to the vacuolar protein-sorting and endocytic pathways. *Molecular biology of the cell*, *11*(10), 3365–3380.

Asaoka, Y., Nagai, Y., Namae, M., Furutani-Seiki, M., & Nishina, H. (2016). SLC7 family transporters control the establishment of left-right asymmetry during organogenesis in medaka by activating mTOR signaling. *Biochemical and biophysical research communications*, *474*(1), 146–153

Babst, M., Katzmann, D.J., Snyder, W.B., Wendland, B., and Emr, S.D. (2002). Endosome- associated complex, ESCRT-II, recruits transport machinery for protein sorting at the multivesicular body. *Dev. Cell 3*, 283–289.

Babst, M. (2011). MVB vesicle formation: ESCRT-dependent, ESCRT-independent and everything in between. *Curr. Opin. Cell Biol. 23*, 452–457.

Babst, M., and Odorizzi G. (2013). The balance of protein expression and degradation: An ESCRTs point of view. *Curr. Opin. Cell Biol. 25*, 489–494.

Babst, M. (2014). Quality control at the plasma membrane: one mechanism does not fit

all. *J. Cell Biol*. *205*, 11–20.

Babst, M. (2020). Regulation of nutrient transporters by metabolic and environmental stresses. *Curr. Opin. Cell Biol. 65*, 35–41.

Bahr, B. A., & Bendiske, J. (2002). The neuropathogenic contributions of lysosomal dysfunction. *Journal of neurochemistry*, *83*(3), 481–489.

Balderhaar, H.J.K., and Ungermann, C. (2013). CORVET and HOPS tethering complexes – coordinators of endosome and lysosome fusion. *J. Cell Sci. 126*, 1307–1316.

Balch, W. E., Morimoto, R. I., Dillin, A., & Kelly, J. W. (2008). Adapting proteostasis for disease intervention. *Science (New York, N.Y.)*, *319*(5865), 916–919.

Ballabio, A. (2016). The awesome lysosome. *EMBO molecular medicine*, *8*(2), 73–76.

Ballabio, A., & Bonifacino, J.,S. (2020). Lysosomes as dynamic regulators of cell and organismal homeostasis. *Nat Rev Mol Cell Biol*. *21*, 101-118.

Bassett, D. E., Jr, Basrai, M. A., Connelly, C., Hyland, K. M., Kitagawa, K., Mayer, M. L., Morrow, D. M., Page, A. M., Resto, V. A., Skibbens, R. V., & Hieter, P. (1996). Exploiting the complete yeast genome sequence. *Current opinion in genetics & development*, *6*(6), 763–766.

Beugnet, A., Tee, A. R., Taylor, P. M., & Proud, C. G. (2003). Regulation of targets of mTOR (mammalian target of rapamycin) signalling by intracellular amino acid availability. *The Biochemical journal*, *372*(Pt 2), 555–566.

Blanc, C., Charette, S.J., Mattei, S., Aubry, L., Smith, E.W., Cosson, P., and Letourneur, F. (2009). Dictyostelium Tom1 participates to an ancestral ESCRT-0 complex. *Traffic 10*,161–171.

Blondel, M.O., Morvan, J., Dupré, S., Urban-Grimal, D., Haguenauer-Tsapis, R., and Volland, C. (2004). Direct sorting of the yeast uracil permease to the endosomal system is controlled by uracil binding and Rsp5p-dependent ubiquitylation. *Mol. Biol. Cell 15*, 883–895.

Borkovich, K.A., Farrelly, F.W., Finkelstein, D.B., Taulien, J., and Lindquist, S. (1989). hsp82 is an essential protein that is required in higher concentrations for growth of cells at higher temperatures. *Mol. Biol. Cell 9*, 3919–3930.

Bukau, B., Weissman, J., Horwich, A. (2006) Molecular chaperones and protein quality control. *Cell 125*(3):443-51.

Bowers, K., Piper, S.C., Edeling, M.A., Gray, S.R., Owen, D.J., Lehner, P.J., and Luzio, J.P. (2006). Degradation of endocytosed epidermal growth factor and virally ubiquitinated major histocompatibility complex class I is independent of mammalian ESCRTII. *J. Biol.Chem*. *281*, 5094–5105.

Brett, C.L., and Merz, A.J. (2008). Osmotic regulation of Rab-mediated organelle docking. *Curr Biol. 18*, 1072–1077.

Brett, C.L., Plemel, R.L., Lobingier, B.T., Vignali, M., Fields, S., and Merz, A.J. (2008). Efficient termination of vacuolar Rab GTPase signaling requires coordinated action by

a GAP and a protein kinase. *J Cell Biol. 182*, 1141–1151.

Bryant, N.J., Piper, R.C., Gerrard, S.R., and Stevens, T.H. (1998). Traffic into the prevacuolar/endosomal compartment of *Saccharomyces cerevisiae*: a VPS45-dependent intracellular route and VPS45-independent, endocytic route. *Eur. J. Cell Biol. 76*, 43–52.

Calamini, B., & Morimoto, R. I. (2012). Protein homeostasis as a therapeutic target for diseases of protein conformation. *Current topics in medicinal chemistry*, *12*(22), 2623–2640.

Carmona-Gutierrez, D., Hughes, A. L., Madeo, F., & Ruckenstuhl, C. (2016). The crucial impact of lysosomes in aging and longevity. *Ageing research reviews*, *32*, 2–12.

Castellano, B. M., Thelen, A. M., Moldavski, O., Feltes, M., van der Welle, R. E., Mydock-McGrane, L., Jiang, X., van Eijkeren, R. J., Davis, O. B., Louie, S. M., Perera, R. M., Covey, D. F., Nomura, D. K., Ory, D. S., & Zoncu, R. (2017). Lysosomal cholesterol activates mTORC1 via an SLC38A9-Niemann-Pick C1 signaling complex. *Science (New York, N.Y.)*, *355*(6331), 1306–1311.

Chassefeyre, R., Martínez-Hernández, J., Bertaso, F., Bouquier, N., Blot, B., Laporte, M.,Fraboulet, S., Couté, Y., Devoy, A., Isaacs, A.M., Pernet-Gallay, K., Sadoul, R., Fagni, L., and Goldberg, Y. (2015). Regulation of postsynaptic function by the dementia-related ESCRT-III subunit CHMP2B. *J. Neurosci. 35*, 3155–3173.

Chen, L., and Davis, N.G. (2002). Ubiquitin-independent entry into the yeast recycling pathway.*Traffic* 3, 110–123.

Chen Y, Lippincott-Schwartz J. (2015) Selective visualization of GLUT4 storage vesicles and associated Rab proteins using IRAP-pHluorin. *Methods Mol Biol*. 1298,173-9

Cohen, L. D., & Ziv, N. E. (2017). Recent insights on principles of synaptic protein degradation. *F1000Research*, *6*, 675.

Cohen, L. D., Zuchman, R., Sorokina, O., Müller, A., Dieterich, D. C., Armstrong, J. D., Ziv, T., & Ziv, N. E. (2013). Metabolic turnover of synaptic proteins: kinetics, interdependencies and implications for synaptic maintenance. *PloS one*, *8*(5), e63191

Cooper, T. G., & Bossinger, J. (1976). Selective inhibition of protein synthesis initiation in Saccharomyces cerevisiae by low concentrations of cycloheximide. *The Journal of biological chemistry*, *251*(22), 7278–7280.

Dai, Q., Escobar, G.P., Hakala, K.W., Lambert, J.M., Weintraub, S.T., Lindsey, M.L. (2008) The left ventricle proteome differentiates middle-aged and old left ventricles in mice. *J Proteome Res. 7(2)*, 756-65

David, D. C., Ollikainen, N., Trinidad, J. C., Cary, M. P., Burlingame, A. L., & Kenyon, C. (2010). Widespread protein aggregation as an inherent part of aging in C. elegans. *PLoS biology*, *8*(8), e1000450.

Davis, N.G., Horecka, J.L., and Sprague Jr, G.F. (1993). Cis- and trans- acting functions required for endocytosis of the yeast pheromone receptors. *J. Cell Biol. 122*, 53–65.

Dobson, L., Reményi, I., & Tusnády, G. E. (2015). The human transmembrane proteome. *Biology direct*, *10*, 31.

Dores, M.R., and Trejo, J. (2019). Endo-lysosomal sorting of G-protein-coupled receptors by ubiquitin: Diverse pathways for G-protein-coupled receptor destruction and beyond. *Traffic 20*, 101–109.

Du, Z., Valtierra, S., Cardona, L. R., Dunne, S. F., Luan, C. H., & Li, L. (2019). Identifying Anti-prion Chemical Compounds Using a Newly Established Yeast High-Throughput Screening System. *Cell chemical biology*, *26*(12), 1664–1680.e4.

Dujon, B., Sherman, D., Fischer, G., Durrens, P., Casaregola, S., Lafontaine, I., De Montigny, J., Marck, C., Neuvéglise, C., Talla, E., Goffard, N., Frangeul, L., Aigle, M., Anthouard, V., Babour, A., Barbe, V., Barnay, S., Blanchin, S., Beckerich, J. M., Beyne, E., … Souciet, J. L. (2004). Genome evolution in yeasts. *Nature*, *430*(6995), 35–44.

Edgar, J.R., Eden, E.R., and Futter, C.E. (2014). Hrs- and CD63-dependent competing mechanisms make different sized endosomal intralumenal vesicles. *Traffic. 15*, 197–211.

Eitzen, G., Will, E., Gallwitz, D., Haas, A., and Wickner, W. (2000). Sequential action of two GTPases to promote vacuole docking and fusion. *EMBO J. 19*, 6713–6720.

Elmonem, M. A., Veys, K. R., Soliman, N. A., van Dyck, M., van den Heuvel, L. P., & Levtchenko, E. (2016). Cystinosis: a review. *Orphanet journal of rare diseases*, *11*, 47.

Fagerberg, L., Jonasson, K., von Heijne, G., Uhlén, M., and Berglund, L. (2010). Prediction of the human membrane proteome. *Proteomics 10*, 1141–1149.

Ferguson, S.M. (2015). Beyond indigestion: emerging roles for lysosome-based signaling in human disease. *Curr. Opin. Cell Biol. 35*, 59–68.

Filimonenko, M., Stuffers, S., Raiborg, C., Yamamoto, A., Malerød, L., Fisher, E. M., Isaacs, A., Brech, A., Stenmark, H., & Simonsen, A. (2007). Functional multivesicular bodies are required for autophagic clearance of protein aggregates associated with neurodegenerative disease. *The Journal of cell biology*, *179*(3), 485–500.

Fotiadis D, Kanai Y, Palacín M. (2013) The SLC3 and SLC7 families of amino acid transporters. *Mol Aspects Med. 34, 139-58.*

Franzmann, T. M., Jahnel, M., Pozniakovsky, A., Mahamid, J., Holehouse, A. S., Nüske, E., Richter, D., Baumeister, W., Grill, S. W., Pappu, R. V., Hyman, A. A., & Alberti, S. (2018). Phase separation of a yeast prion protein promotes cellular fitness. *Science (New York, N.Y.)*, *359*(6371), eaao5654.

Fratti, R.A., Jun, Y., Merz, A.J., Margolis, N., and Wickner, W.T. (2004). Interdependent assembly of specific regulatory lipids and membrane fusion proteins into the vertex ring domain of docked vacuoles. *J Cell Biol. 167*, 1087–1098.

Galaris, D., Barbouti, A., & Pantopoulos, K. (2019). Iron homeostasis and oxidative stress: An intimate relationship. *Biochimica et biophysica acta. Molecular cell research*, *1866*(12), 118535.

Gao, J., Reggiori, F., and Ungermann, C. (2018). A novel in vitro assay reveals SNARE topology and the role of Ykt6 in autophagosomes fusion with vacuoles. *J. Cell Biol. 217*, 3670– 3682.

Ghaddar, K., Merhi, A., Saliba, E., Krammer, E.M., Prévost, M., and André, B. (2014). Substrate-induced ubiquitylation and endocytosis of yeast amino acid permeases. *Mol. Cell Biol. 34*, 4447–4463.

Giaever, G., Chu, A. M., Ni, L., Connelly, C., Riles, L., Véronneau, S., Dow, S., Lucau-Danila, A., Anderson, K., André, B., Arkin, A. P., Astromoff, A., El-Bakkoury, M., Bangham, R., Benito, R., Brachat, S., Campanaro, S., Curtiss, M., Davis, K., Deutschbauer, A., … Johnston, M. (2002). Functional profiling of the Saccharomyces cerevisiae genome. *Nature*, *418*(6896), 387–391.

Gournas, C., Saliba, E., Krammer, E.M., Barthelemy, C., Prévost, M., and André, B. (2017). Transition of yeast Can1 transporter to the inward-facing state unveils an *a*-arrestin target sequence promoting its ubiquitylation and endocytosis. *Mol. Biol. Cell 28*, 2819–2832.

Grimsey, N. J., Aguilar, B., Smith, T. H., Le, P., Soohoo, A. L., Puthenveedu, M. A., Nizet, V., & Trejo, J. (2015). Ubiquitin plays an atypical role in GPCR-induced p38 MAP kinase activation on endosomes. *The Journal of cell biology*, *210*(7), 1117–1131.

Guiney, E.L., Klecker, T., and Emr, S.D. (2016). Identification of the endocytic sorting signal recognized by the Art1-Rsp5 ubiquitin ligase complex. *Mol. Biol. Cell 27*, 4043–4054.

Haas, A., Scheglmann, D., Lazar, T., Gallwitz, D., and Wickner, W. (1995). The GTPase Ypt7p of *Saccharomyces cerevisiae* is required on both partner vacuoles for the homotypic fusion step of vacuole inheritance. *EMBO J. 14*, 5258–5270.

Häfliger, P., & Charles, R. P. (2019). The L-Type Amino Acid Transporter LAT1-An Emerging Target in Cancer. *International journal of molecular sciences*, *20*(10), 2428.

Hanson, P.I., and Cashikar, A. (2012). Multivesicular body morphogenesis. *Annu. Rev. Cell Dev.Biol. 28*, 337–362.

Hatakeyama, R., Péli-Gulli, M.-P., Hu, Z., Jaquenoud, M., Miguel, G., Osuna, G., Sardu, A., Dengjel, J., and De Virgilio, C. (2019). Spatially distinct pools of TORC1 balance protein homeostasis. *Mol. Cell 73*, 325–338.

Henne, W.M., Buchkovich, N.J., and Emr, S.D. (2011). The ESCRT pathway. *Dev. Cell 21*, 77–91.

Hetz, C., & Saxena, S. (2017). ER stress and the unfolded protein response in neurodegeneration. *Nature reviews. Neurology*, *13*(8), 477–491.

Hewitt E. W. (2003). The MHC class I antigen presentation pathway: strategies for viral immune evasion. *Immunology*, *110*(2), 163–169.

Hicke, L., and Riezman, H. (1996). Ubiquitination of a yeast plasma membrane receptor signals its ligand-stimulated endocytosis. *Cell 84*, 277–287.

Hipp, M.S., Kasturi, P. & Hartl, F.U. (2019). The proteostasis network and its decline in ageing. *Nat Rev Mol Cell Biol 20*, 421–435

Hislop, J.N., and von Zastrow, M. (2011). Role of ubiquitination in endocytic trafficking of G- protein-coupled receptors. *Traffic 12*, 137–148.

Höhfeld, J., & Hoppe, T. (2018). Ub and Down: Ubiquitin Exercise for the Elderly. *Trends in cell biology*, *28*(7), 512–522.

Homma, T., & Fujii, J. (2015). Application of Glutathione as Anti-Oxidative and Anti-Aging Drugs. *Current drug metabolism*, *16*(7), 560–571.

Hu, H., & Sun, S. C. (2016). Ubiquitin signaling in immune responses. *Cell research*, *26*(4), 457–483.

Huh, W.K., Falvo, J.V., Gerke, L.C., Carroll, A.S., Howson, R.W., Weissman, J.S., and O'Shea,E.K. (2003). Global analysis of protein localization in budding yeast. *Nature 425*, 686-691.

Hurley, J. H. (2010). The ESCRT complexes. *Critical reviews in biochemistry and molecular biology*, *45*(6), 463–487.

Hurley, J.H. (2015) ESCRTs are everywhere. *EMBO J. 34*, 2398–2407.

Ivashov, V., Zimmer, J., Schwabl, S., Kahlhofer, J., Weys, S., Gstir, R., Jakschitz, T., Kremser, L., Bonn, G. K., Lindner, H., Huber, L. A., Leon, S., Schmidt, O., & Teis, D. (2020). Complementary α-arrestin-ubiquitin ligase complexes control nutrient transporter endocytosis in response to amino acids. *eLife*, *9*, e58246.

Jones, C.B., Ott, E.M., Keener, J.M., Curtiss, M., Sandrin, V., and Babst, M. (2012). Regulation of membrane protein degradation by starvation-response pathways. *Traffic 13*, 468–482.

Juan, T., and Fürthauer, M. (2018). Biogenesis and function of ESCRT-dependent extracellular vesicles. *Semin. Cell Dev. Biol. 74*, 66–77.

Karim, M.A., Samyn, D.R., Mattie, S., and Brett, C.L. (2018a). Distinct features of multivesicular body-lysosome fusion revealed by a new cell-free content-mixing assay. *Traffic 19*, 138– 149.

Karim, M.A., McNally, E.K., Samyn, D.R., Mattie, S., and Brett, C.L. (2018b). Rab-effector-kinase interplay modulates intralumenal fragment formation during vacuole fusion. *Dev. Cell 47*, 80–97.

Katzmann, D.J., Babst, M., and Emr, S.D. (2001). Ubiquitin-dependent sorting into the multivesicular body pathway requires the function of a conserved endosomal protein sorting complex, ESCRT-I. *Cell 106*, 145–155.

Katzmann, D.J., Odorizzi, G., and Emr, S.D. (2002). Receptor downregulation and multivesicular-body sorting. *Nat. Rev. Mol. Cell Biol. 3*, 893–905.

Katzmann, D.J., Stefan, C.J., Babst, M., and Emr, S.D. (2003). Vps27 recruits ESCRT machinery to endosomes during MVB sorting. *J. Cell Biol. 162*, 413–423.

Katzmann, D.J., Sarkar, S., Chu, T., Audhya, A., and Emr, S.D. (2004). Multivesicular body

sorting: Ubiquitin ligase Rsp5 is required for the modification and sorting of carboxypeptidase S. *Mol. Biol. Cell 15*, 468–480.

Kaul, Z., and Chakrabarti, O. (2017). Endosomal complexes required for ESCRTing cells toward death during neurogenesis, neurodevelopment and neurodegeneration. *Traffic 19*, 485– 495.

Keener, J.M., and Babst, M. (2013). Quality control and substrate-dependent downregulation of the nutrient transporter Fur4. *Traffic 14*, 412–427.

Keller, K., Strube, M., & Mueckler, M. (1989). Functional expression of the human HepG2 and rat adipocyte glucose transporters in Xenopus oocytes. Comparison of kinetic parameters. *The Journal of biological chemistry*, *264*(32), 18884–18889.

Klionsky, D. J., Cuervo, A. M., Dunn, W. A., Jr, Levine, B., van der Klei, I., & Seglen, P. O. (2007). How shall I eat thee?. *Autophagy*, *3*(5), 413–416.

Komatsu, M., Waguri, S., Chiba, T., Murata, S., Iwata, J., Tanida, I., Ueno, T., Koike, M., Uchiyama, Y., Kominami, E., & Tanaka, K. (2006). Loss of autophagy in the central nervous system causes neurodegeneration in mice. *Nature*, *441*(7095), 880–884.

Kosicek, M., Gudelj, I., Horvatic, A., Jovic, T., Vuckovic, F., Lauc, G., Hecimovic, S. (2018) N-glycome of the Lysosomal Glycocalyx is Altered in Niemann-Pick Type C Disease (NPC) *Model Cells. Mol Cell Proteomics, 17(4),* 631-642.

Koumanov, F., Pereira, V.J., Whitley, P.R., and Holman, G.D. (2012). GLUT4 traffic through an ESCRT-III-dependent sorting compartment in adipocytes. *PLoS One 7*, e44141.

Kroemer, G., & Levine, B. (2008). Autophagic cell death: the story of a misnomer. *Nature reviews. Molecular cell biology*, *9*(12), 1004–1010. https://doi.org/10.1038/nrm2529

Labbadia, J., & Morimoto, R. I. (2015). The biology of proteostasis in aging and disease. *Annual review of biochemistry*, *84*, 435–464.

Latif, N., Sarathchandra, P., Taylor, P. M., Antoniw, J., & Yacoub, M. H. (2005). Molecules mediating cell-ECM and cell-cell communication in human heart valves. *Cell biochemistry and biophysics*, *43*(2), 275–287.

Lee, S., Ho, H.-C., Tumolo, J.M., Hsu, P.-C., and MacGurn, J.A. (2019). Methionine triggers Ppz- mediated dephosphorylation of Art1 to promote cargo-specific endocytosis. *J. Cell Biol. 218*, 977–992.

Lee, S. R., Bar-Noy, S., Kwon, J., Levine, R. L., Stadtman, T. C., & Rhee, S. G. (2000). Mammalian thioredoxin reductase: oxidation of the C-terminal cysteine/selenocysteine active site forms a thioselenide, and replacement of selenium with sulfur markedly reduces catalytic activity. *Proceedings of the National Academy of Sciences of the United States of America*, *97*(6), 2521–2526.

Lee, S., Tumolo, J. M., Ehlinger, A. C., Jernigan, K. K., Qualls-Histed, S. J., Hsu, P. C., McDonald, W. H., Chazin, W. J., & MacGurn, J. A. (2017). Ubiquitin turnover and endocytic trafficking in yeast are regulated by Ser57 phosphorylation of ubiquitin. *eLife*, *6*, e29176.

Leung, K.F., Dacks, J.B., and Field, M.C. (2008). Evolution of the multivesicular body ESCRT machinery; retention across the eukaryotic lineage. *Traffic 9*, 1698–1716.

Lewis, M.J., and Pelham, H.R. (2009). Inefficient quality control of thermosensitive proteins on the plasma membrane. *PLoS One 4*, e5038.

Li, L., & Kaplan, J. (1998). Defects in the yeast high affinity iron transport system result in increased metal sensitivity because of the increased expression of transporters with a broad transition metal specificity. *The Journal of biological chemistry*, *273*(35), 22181–22187.

Li, M., Rong, Y., Chuang, Y., Peng, D., and Emr., S.D. (2015a). Ubiquitin-dependent lysosomal membrane protein sorting and degradation. *Mol. Cell 57*, 467–478.

Li, M., Koshi, T., and Emr, S.D. (2015b). Membrane-anchored ubiquitin ligase complex is required for the turnover of lysosomal membrane proteins. *J. Cell Biol. 211*, 639–652.

Li, S.C., and Kane, P.M. (2009). The yeast lysosome-like vacuole: endpoint and crossroads. *Biochim. Biophys. Acta. 1793*, 650–663.

Lin, C.H., MacGurn, J.A., Chu, T., Stefan, C.J., and Emr, S.D. (2008). Arrestin-related ubiquitin- ligase adaptors regulate endocytosis and protein turnover at the cell surface. *Cell 135*, 714–725.

Lin, Z., Zhao, D., Wang, Y., Zhao, W., Yin, X., Zhou, X., Zhang, Z., & Yang, L. (2015). Downregulation of β-Soluble N-Ethylmaleimide-Sensitive Factor Attachment Protein: Proteomics-Based Identification in Early-Stage Prion Disease. *Neuro-degenerative diseases*, *15*(4), 193–201.

Liu, C., Lou, W., Yang, J. C., Liu, L., Armstrong, C. M., Lombard, A. P., Zhao, R., Noel, O., Tepper, C. G., Chen, H. W., Dall'Era, M., Evans, C. P., & Gao, A. C. (2018). Proteostasis by STUB1/HSP70 complex controls sensitivity to androgen receptor targeted therapy in advanced prostate cancer. *Nature communications*, *9*(1), 4700.

Lobert, V.H., and Stenmark, H. (2011). Cell polarity and migration: emerging role for the endosomal sorting machinery. *Physiology (Bethesda) 26*, 171–180.

Loewith, R., & Hall, M. N. (2011). Target of rapamycin (TOR) in nutrient signaling and growth control. *Genetics*, *189*(4), 1177–1201.

Longtine, M.S., Mckenzie III, A., Demarini, D.J., Shah, N.G., Wach, A., Brachat, A., Philippsen, P., and Pringle, J.R. (1998). Additional modules for versatile and economical PCR-based gene deletion and modification in Saccharomyces cerevisiae. *Yeast 14*, 953–961.

Luzio, J. P., Pryor, P. R., & Bright, N. A. (2007). Lysosomes: fusion and function. *Nature reviews. Molecular cell biology*, *8*(8), 622–632.

MacDonald, C., Stringer, D.K., and Piper, R.C. (2012). Sna3 is an Rsp5 adaptor protein that relies on ubiquitination for its MVB sorting. *Traffic 13*, 586–598.

MacGurn, J.A., Hsu, P.C., Smolka, M.B., and Emr, S.D. (2011). TORC1 regulates

endocytosis via Npr1-mediated phosphoinhibition of a ubiquitin ligase adaptor. *Cell 147*, 1104–1117.

MacGurn, J.A., Hsu, P.C., and Emr, S.D. (2012). Ubiquitin and membrane protein turnover: from cradle to grave. Annu. Rev. Biochem. *81*, 231–259.

Mageswaran, S.K., Johnson, N.K., Odorizzi, G., and Babst, M. (2015). Constitutively active ESCRT-II suppresses the MVB-sorting phenotype of ESCRT-0 and ESCRT-I mutants. *Mol. Biol. Cell 26*, 554–5

Manolson, M. F., Proteau, D., & Jones, E. W. (1992). Evidence for a conserved 95-120 kDa subunit associated with and essential for activity of V-ATPases. *The Journal of experimental biology*, *172*, 105–112.

Manteghi, S., Gingras, M.-C., Kharitidi, D., Galarneau, L., Marques, M., Yan, M., Cencic, R., Robert, F., Paquet, M., Witcher, M., Pelletier, J., and Pause, A. (2016). Haploinsufficiency of the ESCRT component HD-PTP predisposes to cancer. *Cell Rep. 15*, 1893–1900.

Marigomez, J. A., Vega, M. M., Cajaraville, M. P., & Angulo, E. (1989). Quantitative responses of the digestive-lysosomal system of winkles to sublethal concentrations of cadmium. *Cellular and molecular biology*, *35*(5), 555–562.

Matsuura-Tokita, K., Takeuchi, M., Ichihara, A., Mikuriya, K., & Nakano, A. (2006). Live imaging of yeast Golgi cisternal maturation. *Nature*, *441*(7096), 1007–1010.

Mattie, S., McNally, E.K., Karim, M.A., Vali, H., and Brett, C.L. (2017). How and why intralumenal membrane fragments form during vacuolar lysosome fusion. *Mol. Biol. Cell 28*, 309–321.

McLendon, P. M., & Robbins, J. (2015). Proteotoxicity and cardiac dysfunction. *Circulation research*, *116*(11), 1863–1882.

McNally, E.K., Karim, M.A., and Brett, C.L. (2017). Selective Lysosomal Transporter Degradation by Organelle Membrane Fusion. *Dev. Cell 40*, 151–167.

McNally, E.K., and Brett, C.L. (2018). The intralumenal fragment pathway mediates ESCRT- independent surface transporter down-regulation. *Nat. Commun. 9*, 5358.

McNatt, M.W., McKittrick, I., West, M., and Odorizzi, G. (2007). Direct binding to Rsp5 mediates ubiquitin-independent sorting of Sna3 via the multivesicular body pathway. *Mol. Biol. Cell 18*, 697–706.

Miesenböck, G., De Angelis, D. A., & Rothman, J. E. (1998). Visualizing secretion and synaptic transmission with pH-sensitive green fluorescent proteins. *Nature*, *394*(6689), 192–195

Miledi, R., Eusebi, F., Martínez-Torres, A., Palma, E., & Trettel, F. (2002). Expression of functional neurotransmitter receptors in Xenopus oocytes after injection of human brain membranes. *Proc. of the Nat. Aca. of Sci. of the U.S.A*, *99*(20), 13238–13242.

Monti, P., Bosco, B., Gomes, S., Saraiva, L., Fronza, G., & Inga, A. (2019). Yeast As a Chassis for Developing Functional Assays to Study Human P53. *Journal of visualized experiments : JoVE*, (150), 10.3791/59071.

Napolitano, G., and Ballabio, A. (2016). TFEB at a glance. *J. Cell Sci. 129*, 2475–2481.

Nickerson, D.P., Brett, C.L., and Merz, A.J. (2009). Vps-C complexes: gatekeepers of endolysosomal traffic. *Curr. Opin. Cell Biol. 21*, 543–551.

Nikko, E., and Pelham, H.R. (2009). Arrestin-mediated endocytosis of yeast plasma membrane transporters. *Traffic 10*, 1856–1867.

Novikoff, A.B., Beaufay, H., and De Duve, C. (1956). Electron microscopy of lysosome-rich fractions from rat liver. J. Biophys. Biochem. Cytol. *2*, 179–184.
Odorizzi, G., Babst, M., and Emr, S.D. (1998). Fab1p PtdIns(3)P5-kinase function essential for protein sorting in the multivesicular body. *Cell 95*, 847–858.

Olivares-Marin, I. K., González-Hernández, J. C., Regalado-Gonzalez, C., & Madrigal-Perez, L. A. (2018). Saccharomyces cerevisiae Exponential Growth Kinetics in Batch Culture to Analyze Respiratory and Fermentative Metabolism. *Journal of visualized experiments : JoVE*, (139), 58192.

Otegui, M.S. (2018). ESCRT-mediated sorting and intralumenal vesicle concatenation in plants. *Biochem. Soc. Trans. 46*, 537–545.

Pal D, Eisenberg D. (2005) Inference of protein function from protein structure. *Structure. 13*(1), 121-30.

Palacios, F., Tushir, J.S., Fujita, Y., and D'Souza-Schorey, C. (2005). Lysosomal targeting of E-cadherin: a unique mechanism for the down-regulation of cell-cell adhesion during epithelial to mesenchymal tranasitions. *Mol. Cell Biol*. *25*, 389–402.

Pataer, A., Ozpolat, B., Shao, R., Cashman, N. R., Plotkin, S. S., Samuel, C. E., Lin, S. H., Kabil, N. N., Wang, J., Majidi, M., Fang, B., Roth, J. A., Vaporciyan, A. A., Wistuba, I. I., Hung, M. C., & Swisher, S. G. (2020). Therapeutic targeting of the PI4K2A/PKR lysosome network is critical for misfolded protein clearance and survival in cancer cells. *Oncogene*, *39*(4), 801–813.

Parkinson, M.D., Piper, S.C., Bright, N.A., Evans, J.L., Boname, J.M., Bowers, K., Lehner, P.J., and Luzio, J.P. (2015). A non-canonical ESCRT pathway, including histidine domain phosphotyrosine phosphatase (HD-PTP), is used for down-regulation of virally ubiquitinated MHC class I. *Biochem. J. 471*, 79–88.

Piper, R.C., Cooper, A.A., Yang, H., and Stevens, T.H. (1995). VPS27 controls vacuolar and endocytic traffic through a prevacuolar compartment in *Saccharomyces cerevisiae*. *J. Cell Biol., 131*, 603–617.

Platt, F. M., d'Azzo, A., Davidson, B. L., Neufeld, E. F., & Tifft, C. J. (2018). Lysosomal storage diseases. *Nature Reviews Disease Primers*, *4*(1), 1-25.

Prosser, D.C., Whitworth, K., and Wendland, B. (2010). Quantitative analysis of endocytosis with cytoplasmic pHluorin chimeras. *Traffic*, *11*, 1141–1150.

Raiborg, C., and Stenmark, H. (2009). The ESCRT machinery in endosomal sorting of ubiquitylated membrane proteins. *Nature*, *458*, 445–452.

Rajapakse, D., Curtis, T., Chen, M., & Xu, H. (2017). Zinc Protects Oxidative Stress-Induced RPE Death by Reducing Mitochondrial Damage and Preventing Lysosome Rupture. *Oxidative medicine and cellular longevity*, *2017*, 6926485.

Raymond, C.K., Howald-Stevenson, I., Vater, C.A., and Stevens, T.H. (1992). Morphological classification of the yeast vacuolar protein sorting mutants: evidence for a prevacuolar compartment in class E vps mutants. *Mol. Biol. Cell 3*, 1389–1402.

Rayner, S. L., Morsch, M., Molloy, M. P., Shi, B., Chung, R., & Lee, A. (2019). Using proteomics to identify ubiquitin ligase-substrate pairs: how novel methods may unveil therapeutic targets for neurodegenerative diseases. *CMLS*, *76*(13), 2499–2510.

Reggiori, F., and Pelham, H.R. (2001). Sorting of proteins into multivesicular bodies: ubiquitin-dependent and -independent targeting. *EMBO J. 20*, 5176–5186.

Ren, J., Kee, Y., Huibregtse, J. M., & Piper, R. C. (2007). Hse1, a component of the yeast Hrs-STAM ubiquitin-sorting complex, associates with ubiquitin peptidases and a ligase to control sorting efficiency into multivesicular bodies. *Mol. Biol. of the Cell*, *18*(1), 324–335.

Ren, X., and Hurley, J.H. (2010). VHS domains of ESCRT-0 cooperate in high-avidity binding to polyubiquitinated cargo. *EMBO J. 29*, 1045–1054.

Ren, X., and Hurley, J.H. (2011). Structural basis for endosomal recruitment of ESCRT-I by ESCRT-0 in yeast. EMBO J. *30*, 2130–2139.

Robinson, J.S., Klionsky, D.J., Banta, L.M., and Emr, S.D. (1988). Protein sorting in *Saccharomyces cerevisiae*: isolation of mutants defective in the delivery and processing of multiple vacuolar hydrolases. *Mol. Cell Biol. 8*, 4936–4948.

Roberts, G. G., & Hudson, A. P. (2006). Transcriptome profiling of Saccharomyces cerevisiae during a transition from fermentative to glycerol-based respiratory growth reveals extensive metabolic and structural remodeling. *Molecular genetics and genomics : MGG*, *276*(2), 170–186.

Rodahl, L.M., Stuffers, S., Lobert, V.H., and Stenmark, H. (2009). The role of ESCRT proteins in attenuation of cell signalling. *Biochem. Soc. Trans. 37*, 137–142.

Roh, H. C., Collier, S., Guthrie, J., Robertson, J. D., & Kornfeld, K. (2012). Lysosome-related organelles in intestinal cells are a zinc storage site in C. elegans. *Cell metabolism*, *15*(1), 88–99.

Ron, D., Walter, P. (2007) Signal integration in the endoplasmic reticulum unfolded protein response. *Nat Rev Mol Cell Biol. 8*(7),519-529.

Roth, A. F., Sullivan, D. M., & Davis, N. G. (1998). A large PEST-like sequence directs the ubiquitination, endocytosis, and vacuolar degradation of the yeast a-factor receptor. *The Journal of cell biology*, *142*(4), 949–961.

Roth, R. M., & Dampier, C. (1972). Dependence of ribonucleic acid synthesis on continuous protein synthesis in yeast. *Journal of bacteriology*, *109*(2), 773–779.

Rothman, J. E., & Wieland, F. T. (1996). Protein sorting by transport vesicles. *Science (New York, N.Y.)*, *272*(5259), 227–234.

Ruggiano, A., Foresti, O., & Carvalho, P. (2014). Quality control: ER-associated degradation: protein quality control and beyond. *The Journal of cell biology*, *204*(6), 869–879.

Ruiz, S. J., van 't Klooster, J. S., Bianchi, F., & Poolman, B. (2020). Growth Inhibition by Amino Acids in *Saccharomyces cerevisiae*. *Microorganisms*, *9*(1), 7.

Rusten, T. E., & Simonsen, A. (2008). ESCRT functions in autophagy and associated disease. *Cell cycle (Georgetown, Tex.)*, *7*(9), 1166–1172.

Salas-Moreno, M., Contreras-Puentes, N., Rodríguez-Cavallo, E., Jorrín-Novo, J., Marrugo-Negrete, J., & Méndez-Cuadro, D. (2019). Protein Carbonylation As a Biomarker of Heavy Metal, Cd and Pb, Damage in *Paspalum fasciculatum* Willd. ex Flüggé. *Plants (Basel, Switzerland)*, *8*(11), 513.

Sasser, T. L., Padolina, M., & Fratti, R. A. (2012). The yeast vacuolar ABC transporter Ybt1p regulates membrane fusion through Ca2+ transport modulation. *The Biochemical journal*, *448*(3), 365–372.

Sasser, T. L., Lawrence, G., Karunakaran, S., Brown, C., & Fratti, R. A. (2013). The yeast ATP-binding cassette (ABC) transporter Ycf1p enhances the recruitment of the soluble SNARE Vam7p to vacuoles for efficient membrane fusion. *The Journal of biological chemistry*, *288*(25), 18300–18310.

Savitski, M. M., Zinn, N., Faelth-Savitski, M., Poeckel, D., Gade, S., Becher, I., Muelbaier, M., Wagner, A. J., Strohmer, K., Werner, T., Melchert, S., Petretich, M., Rutkowska, A., Vappiani, J., Franken, H., Steidel, M., Sweetman, G. M., Gilan, O., Lam, E., Dawson, M. A., … Bantscheff, M. (2018). Multiplexed Proteome Dynamics Profiling Reveals Mechanisms Controlling Protein Homeostasis. *Cell*, *173*(1), 260–274.e25.

Saksena, S., and Emr, S.D. (2009). ESCRTs and human disease. *Biochem. Soc. Trans. 37*, 167– 172.

Sardana, R., Zhu, L., and Emr, S.D. (2019). Rsp5 ubiquitin ligase-mediated quality control system clears membrane proteins mistargeted to the vacuole membrane. *J. Cell Biol. 218*, 234–250.

Settembre, C., Fraldi, A., Medina, D. L., & Ballabio, A. (2013). Signals from the lysosome: a control centre for cellular clearance and energy metabolism. *Nature reviews. Molecular cell biology*, *14*(5), 283–296.

Shaw, J.D., Hama, H., Sohrabi, F., DeWald, D.B., and Wendland, B. (2003). PtIns(3,5)P2 is required for delivery of endocytic cargo into the multivesicular body. *Traffic* 4, 479–490.

Shields, S.B., Oestreich, A.J., Winistorfer, S., Nguyen, D., Payne, J.A., Katzmann, D.J., and Piper, R. (2009). ESCRT ubiquitin-binding domains function cooperatively during MVB cargo sorting. *J. Cell Biol. 185*, 213–224.

Shivapurkar, N., Wilson, M. J., & Poirier, L. A. (1984). Hypomethylation of DNA in ethionine-fed rats. *Carcinogenesis*, *5*(8), 989–992.

Silverman, J.S., Muratore, K.A., and Bangs, J.D. (2013). Characterization of the late endosomal ESCRT machinery in *Trypanosoma brucei. Traffic 14*, 1078–1090.

Sigismund, S., Avanzato, D., & Lanzetti, L. (2018). Emerging functions of the EGFR in cancer. *Molecular oncology*, *12*(1), 3–20.

Stanley, P., Taniguchi, N., and Aebi, M. (2017). Essentials of Glycobiology, 3rd Edition. *Cold Spring Harbor Laboratory Press.* Chapter 9.

Stuffers, S., Brech, A., and Stenmark, H. (2009a). ESCRT proteins in physiology and disease. *Exp. Cell Res. 315*, 1619–1626.

Stuffers, S., Sem Wegner, C., Stenmark, H., and Brech, A. (2009b). Multivesicular endosome biogenesis in the absence of ESCRTs. *Traffic 10*, 925–937.

Tarassov, K., Messier, V., Landry, C. R., Radinovic, S., Serna Molina, M. M., Shames, I., Malitskaya, Y., Vogel, J., Bussey, H., & Michnick, S. W. (2008). An in vivo map of the yeast protein interactome. *Science (New York, N.Y.)*, *320*(5882), 1465–1470.

Taylor, R. C., & Dillin, A. (2011). Aging as an event of proteostasis collapse. *Cold Spring Harbor perspectives in biology*, *3*(5), a004440.

Teis, D., Saksena, S., Judson, B.L., and Emr, S.D. (2010). ESCRT-II coordinates the assembly of ESCRT-III filaments for cargo sorting and multivesicular body formation. *EMBO J. 29*, 871–883.

ten Broeke, T., Wubbolts, R., & Stoorvogel, W. (2013). MHC class II antigen presentation by dendritic cells regulated through endosomal sorting. *Cold Spring Harbor perspectives in biology*, *5*(12), a016873.

Theos, A.C., Truschel, S.T., Tenza, D., Hurbain, I., Harper, D.C., Berson, J.F., Thomas, P.C., Raposo, G., and Marks, M.S. (2006). A lumenal domain-dependent pathway for sorting to intralumenal vesicles of multivesicular endosomes involved in organelle morphogenesis. *Dev. Cell 10*, 343–354.

Trajkovic, K., Hsu, C., Chiantia, S., Rajendran, L., Wenzel, D., Wieland, F., Schwille, P., Brügger, B., and Simons, M. (2008). Ceramide triggers budding of exosome vesicles into multivesicular endosomes. *Science 319*, 1244–1247.

Urbanowski, J. L., & Piper, R. C. (1999). The iron transporter Fth1p forms a complex with the Fet5 iron oxidase and resides on the vacuolar membrane. *The Journal of biological chemistry*, *274*(53), 38061–38070.

Velasco, I., Tenreiro, S., Calderon, I. L., & André, B. (2004). Saccharomyces cerevisiae Aqr1 is an internal-membrane transporter involved in excretion of amino acids. *Eukaryotic cell*, *3*(6), 1492–1503.

Vida, T. A., & Emr, S. D. (1995). A new vital stain for visualizing vacuolar membrane dynamics and endocytosis in yeast. *The Journal of cell biology*, *128*(5), 779–792.

Vietri, M., Radulovic, M., and Stenmark, H. (2019). The many functions of ESCRTs. *Nat. Rev. Mol. Cell Biol. 21*, 25–42.

Volland, C., Urban-Grimal, D., Géraud, G., and Haguenauer-Tsapis, R. (1994). Endocytosis and degradation of the yeast uracil permease under adverse conditions. *J. Biol. Chem*. *269*, 9833–9841.

Votteler, J., and Sundquist, W.I. (2013). Virus budding and the ESCRT pathway. *Cell Host Microbe 14*, 232–241.

Wang, L., Seeley, E.S., Wickner, W., and Merz, A.J. (2002). Vacuole fusion at a ring of vertex docking sites leaves membrane fragments within the organelle. *Cell 108*, 357–

369.
Wang, L., Merz, A.J., Collins, K.M., and Wickner, W. (2003). Hierarchy of protein assembly at the vertex ring domain for yeast vacuole docking and fusion. *J. Cell Biol. 160*, 365–374.
Wang, S., Thibault, G., and Ng, D.T. (2011). Routing misfolded proteins through the multivesicular body (MVB) pathway protects against proteotoxicity. *J. Biol. Chem. 286*, 29376–29387.
Wang, X., Venable, J., LaPointe, P., Hutt, D. M., Koulov, A. V., Coppinger, J., Gurkan, C., Kellner, W., Matteson, J., Plutner, H., Riordan, J. R., Kelly, J. W., Yates, J. R., 3rd, & Balch, W. E. (2006). Hsp90 cochaperone Aha1 downregulation rescues misfolding of CFTR in cystic fibrosis. *Cell*, *127*(4), 803–815.
Werner-Washburne, M., Stone, D.E., and Craig, E.A. (1987). Complex interactions among members of an essential subfamily of hsp70 genes in *Saccharomyces cerevisiae*. *Mol. Biol. Cell 7*, 2568–2577.
Wickner, W. (2010). Membrane fusion: five lipids, four SNAREs, three chaperones, two nucleotides, and a Rab, all dancing in a ring on yeast vacuoles. *Annu. Rev. Cell Dev. Biol. 26*, 115–136.
Wickner, W., & Haas, A. (2000). Yeast homotypic vacuole fusion: a window on organelle trafficking mechanisms. *Annu. Rev. Biochem.*, *69*, 247–275.
Winkler, M., Kidmose, R. T., Szomek, M., Thaysen, K., Rawson, S., Muench, S. P., Wüstner, D., & Pedersen, B. P. (2019). Structural Insight into Eukaryotic Sterol Transport through Niemann-Pick Type C Proteins. *Cell*, *179*(2), 485–497.e18.
Wosen, J. E., Mukhopadhyay, D., Macaubas, C., & Mellins, E. D. (2018). Epithelial MHC Class II Expression and Its Role in Antigen Presentation in the Gastrointestinal and Respiratory Tracts. *Frontiers in immunology*, *9*, 2144.
Wrasman, K., Alioto, S.L., Zhang, Y., Hoban, K., Khairy, M., Goode, B.L., and Wendland, B. (2018). A flow cytometry-based phenotypic screen to identify novel endocytic factors in Saccharomyces cerevisiae. *G3 (Bethesda) 8*, 1497–1512.
Xu, X. L., Fang, Y., Lee, T. C., Forrest, D., Gregory-Evans, C., Almeida, D., Liu, A., Jhanwar, S. C., Abramson, D. H., & Cobrinik, D. (2009). Retinoblastoma has properties of a cone precursor tumor and depends upon cone-specific MDM2 signaling. *Cell*, *137*(6), 1018–1031
Yang, D., and Hurley, J.H. (2010). Structural role of the Vps4-Vta1 interface in ESCRT-III recycling. *Structure 18*, 976–984.
Yang, X., Zhang, W., Wen, X., Bulinski, P.J., Chomchai, D.A., Arines, F.M., Liu, Y.Y., Sprenger, S., Teis, D., Klionsky, D.J., and Li, M. (2020). TORC1 regulates vacuole membrane composition through ubiquitin- and ESCRT- dependent microautophagy. *J. Cell Biol. 219*, e201902127.
Yeo, S.C., Xu, L., Ren, J., Boulton, V.J., Wagle, M.D., Liu, C., Ren, G., Wong, P., Zahn, R., Sasajala, P., Yang, H., Piper, R.C., and Munn, A.L. (2003). Vps20p and Vta1p

interact with Vps4p and function in multivesicular body sorting and endosomal transport in *Saccharomyces cerevisiae*. *J. Cell Sci. 116*, 3957–3970.

Yofe, I., Weill, U., Meurer, M., Chuartzman, S., Zalckvar, E., Goldman, O., Ben-Dor, S., Schütze, C., Wiedemann, N., Knop, M., Khmelinskii, A., & Schuldiner, M. (2016). One library to make them all: streamlining the creation of yeast libraries via a SWAp-Tag strategy. *Nature methods*, *13*(4), 371–378.

Zavodszky, E., & Hegde, R. S. (2019). Misfolded GPI-anchored proteins are escorted through the secretory pathway by ER-derived factors. *eLife*, *8*, e46740.

Zhang, D., Wu, C. T., Qi, X., Meijering, R. A., Hoogstra-Berends, F., Tadevosyan, A., Cubukcuoglu Deniz, G., Durdu, S., Akar, A. R., Sibon, O. C., Nattel, S., Henning, R. H., & Brundel, B. J. (2014). Activation of histone deacetylase-6 induces contractile dysfunction through derailment of α-tubulin proteostasis in experimental and human atrial fibrillation. *Circulation*, *129*(3), 346–358.

Zhang, Y. X., van Oosterwijk, J. G., Sicinska, E., Moss, S., Remillard, S. P., van Wezel, T., Bühnemann, C., Hassan, A. B., Demetri, G. D., Bovée, J. V., & Wagner, A. J. (2013). Functional profiling of receptor tyrosine kinases and downstream signaling in human chondrosarcomas identifies pathways for rational targeted therapy. *Clinical cancer research: an official journal of the American Association for Cancer Research*, *19*(14), 3796–3807.

Zhao, Y., Macgurn, J.A., Liu, M., and Emr, S. (2013). The ART-Rsp5 ubiquitin ligase network comprises a plasma membrane quality control system that protects yeast cells from proteotoxic stress. *Elife 2*, e00459

Zhou, R., Kabra, R., Olson, D.R., Piper, R.C., and Snyder, P.M. (2010). Hrs controls sorting of the epithelial Na+ channel between endosomal degradation and recycling pathways. *J. Biol. Chem. 285*, 30523–30530.

Zhu, L., Jorgensen, J.R., Li, M., Chuang, Y.S., and Emr, S.D. (2017). ESCRTs function directly on the lysosome membrane to downregulate ubiquitinated lysosomal membrane proteins. *Elife 6*, e26403.